

PA00881

COPY NO. 17

**ANTENNA EVALUATION STUDY**  
**FOR THE**  
**SHUTTLE MULTISPECTRAL RADAR: PHASE II**

NASA CR-  
151538

FINAL REPORT

by

Edgar L. Coffey, III  
Keith R. Carver

prepared for

NASA Johnson Space Center  
Houston, Texas

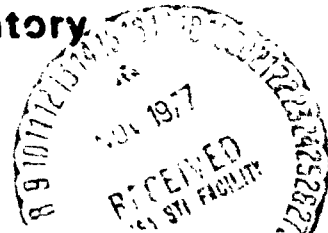
Contract No.  
NAS 9-95471

MAY 1977



**Physical Science Laboratory**

BOX 3548, LAS CRUCES, NEW MEXICO 88003  
AREA (505) 522-4400 TWX 910-983-0541



(NASA-CR-151538) ANTENNA EVALUATION STUDY  
FOR THE SHUTTLE MULTISPECTRAL RADAR, PHASE 2  
Final Report (New Mexico State Univ.) 58 p  
HC A04/MF A01

CSCL 173

N78-10194

Unclas  
53/16 52076

**PA00881**

**ANTENNA EVALUATION STUDY**  
**FOR THE**  
**SHUTTLE MULTISPECTRAL RADAR: PHASE II**

**FINAL REPORT**

**by**

**Edgar L. Coffey, III**  
**Keith R. Carver**

**prepared for**

**NASA Johnson Space Center**  
**Houston, Texas**

**Contract No.**  
**NAS 9-95471**

**MAY 1977**

## TABLE OF CONTENTS

	Page
1.0 INTRODUCTION .....	1
2.0 ANTENNA TEST PANEL SPECIFICATIONS .....	2
2.1 Electrical Specifications .....	2
2.1.1 Electrical Structure .....	7
2.1.2 Frequency of Operation .....	8
2.1.3 Polarization .....	8
2.1.4 Beam Width Switching .....	8
2.1.5 Antenna Gain .....	9
2.1.6 Antenna Insertion Loss .....	9
2.1.7 Antenna VSWR .....	10
2.1.8 Polarization Purity .....	11
2.1.9 Beam Pointing Accuracy .....	11
2.1.10 Side Lobe Level .....	12
2.1.11 Power Handling Requirements .....	12
2.1.12 Other Pattern Requirements .....	12
2.2 Mechanical Specifications .....	13
2.2.1 Mechanical Dimensions .....	13
2.2.2 Weight .....	13
2.2.3 Support Structure .....	13
2.2.4 Mechanical Deformation Testing .....	14
2.2.5 Interface with PSL Deformation Simulator .....	14
2.2.6 Connectors .....	15
2.2.7 Environmental and Stability of Materials .....	15
2.2.8 Folding Mechanism .....	15
3.0 COMPUTER SIMULATION OF MECHANICAL/THERMAL DEFORMATIONS .....	16
3.1 Effects of Errors On Antenna Gain .....	18
3.2 Beam Pointing Errors .....	23
3.3 Main Beam Shape .....	33
3.4 Side Lobe Level .....	33

TABLE OF CONTENTS (Cont'd)

	Page
3.5 Other Antenna Parameters .....	40
3.6 Summary of Computer Predictions .....	40
4.0 FOOTPRINT CONTOUR MAPS OF FIFTEEN SIMULATIONS .....	45

# LIST OF ILLUSTRATIONS

Figure		Page
2.1	Shuttle imaging radar antenna test panel allocation of area .....	5
3.1	Antenna deformation configurations used in the computer model .....	17
3.2	Gain degradation (dB) versus frequency (GHz) for a panel unfolding error of (-1.0, 2.0) cm at (a) 10 degree tilt (b) 50 degree tilt .....	19
3.3	Gain degradation (dB) versus frequency (GHz) for a five cm parabolic bow at (a) 10 degree tilt, (b) 50 degree tilt .....	20
3.4	Gain degradation (dB) versus warp severity at 1.5 GHz and 10° tilt for (a) panel unfolding errors, (b) parabolic bow errors .....	21
3.5	Gain degradation (dB) versus warp severity (cm) for parabolic bow errors at a 10° tilt: (a) 1.5 GHz, (b) 9.0 GHz .....	22
3.6	Beam pointing error (km) versus panel unfolding error (cm) at f = 1.5 GHz for (a) 10° tilt, (b) 50° tilt .....	24
3.7	Beam pointing error (km) versus panel unfolding error (cm) at f = 9.0 GHz for (a) 10° tilt, (b) 50° tilt .....	25
3.8	Azimuthal main beam footprint profile .....	26
3.9	Azimuthal main beam footprint profile .....	27
3.10	Azimuthal main beam footprint profile .....	28
3.11	Azimuthal main beam footprint profile .....	29
3.12	Azimuthal main beam footprint profile .....	30
3.13	Azimuthal main beam footprint profile .....	31
3.14	Azimuthal main beam footprint profile .....	32
3.15	Azimuth beam width (meters) versus warp severity (cm) for panel unfolding errors at 1.5 GHz and 200 km: (a) 10° tilt, (b) 50° tilt .....	34
3.16	Three DB azimuth beam width (meters) vs warp severity (CM) parabolic bow error .....	35
3.17	Azimuth main beam footprint profile .....	36
3.18	Azimuth main beam footprint profile .....	37
3.19	Azimuth main beam footprint profile .....	38
3.20	Azimuth main beam footprint profile .....	39
3.21	Side lobe level (dB) vs frequency (GHz) for panel unfolding errors at (a) 10° tilt, (b) 50° tilt .....	41

# LIST OF ILLUSTRATIONS (Cont'd)

Figure		Page
3.22	Azimuth profile plane side lobe level (dB) versus warp severity for panel unfolding errors at 1.5 GHz: (a) 10° tilt, (b) 50° tilt .....	42
3.23	Azimuth profile plane side lobe level (DB) vs warp severity (CM) (parabolic bow deformation) .....	43
	<b>Fifteen Simulations of Footprint Contour Maps</b>	
4.1	.....	46
4.2	.....	47
4.3	.....	48
4.4	.....	49
4.5	.....	50
4.6	.....	51
4.7	.....	52
4.8	.....	53
4.9	.....	54
4.10	.....	55
4.11	.....	56
4.12	.....	57
4.13	.....	58
4.14	.....	59
4.15	.....	60

# LIST OF TABLES

	Page
Table I. Shuttle Imaging Radar Antenna Test Panel Electrical Specifications .....	3
Table II. Shuttle Imaging Radar Antenna Test Panel Mechanical Specifications .....	6

# LIST OF REFERENCES

Reference		Page
1	From PSL Technical Proposal, Phase II .....	1
2	<u>SERGE Antenna Concept Selection Review Report, NASA</u> Contract NAS9-15363, August 3, 1977 .....	40

## 1.0 INTRODUCTION

This report presents the results of the second phase of the Antenna Evaluation Study for the Shuttle Imaging Radar (SIR). The objectives of Phase II were (1) to complete the specifications for the subarray test panels, (2) to begin a study of the effects of electrical and mechanical tolerance variations on overall SIRA performance, (3) to initiate the development of a mathematical model which adequately describes the array performance and (4) to begin the development of a comprehensive computer program which will eventually simulate the performance characteristics of the antenna in a space-borne environment<sup>1</sup>. Items (2), (3), and (4) were begun in Phase I (ahead of schedule), and because of this, it has been possible to accelerate the Phase II modeling/simulation objectives to the point where simulations of expected mechanical/electrical errors have already been produced.

---

<sup>1</sup>

From PSL Technical Proposal, Phase II.

## 2.0 ANTENNA TEST PANEL SPECIFICATIONS

The purpose of constructing subarray panels is two-fold:

1. To produce realistic simulation and measurement of reduced-size array behavior and to extend this to a prediction of full-size array behavior.
2. To verify the ability of near-field antenna pattern measurement techniques to measure full-scale SIRA characteristics, particularly in gain, beam coincidence, and cross-polarization levels at X-band.

The specifications on these test panels are based on an estimate of the tests and measurements that will be required to obtain the above results. Further constraints are imposed by measurement facility restrictions at PSL (for far-field data) and NBS (for near-field data) and such practical considerations as size, weight, etc. The test panel specifications, predicated on a dual-band, dual-polarized antenna, are given in Tables I and II. Details of each specification and its justification are given below.

### 2.1 Electrical Specifications

At the time these specifications were made, it had been tentatively decided to configure the SIRA as a dual frequency (C- and X-band) and dual polarized antenna. Specifications, therefore, reflect this design and not the later SIR-A/SIR-B philosophy.

TABLE I. Shuttle Imaging Radar Antenna Test Panel Electrical Specifications

1. Electrical structure dimensions shall be 1.83 m by 1.83 m  $\pm$  10%.
2. The antenna shall be dual frequency: 4.75 and 9.6 GHz.
3. The antenna shall have both horizontal and vertical polarization capability at each frequency.
4. There shall be two modules at each frequency (and/or polarization) to replicate beam width switching. (Note 1)
5. The antenna gain using both modules shall be at least 32 dB at 4.75 GHz and 33 dB at 9.6 GHz. Antenna gain shall be optimized within the bounds of other specifications.
6. The total antenna loss (ratio of maximum gain to maximum directivity) shall not exceed 1.5 dB.
7. The VSWR in any mode of operation shall not exceed 1.3:1.
8. For any mode of operation, the cross-polarized component shall be at least -30 dB with respect to the maximum principal polarization component as measured over the entire beam.
9. The electrical beam maximum shall be within  $0.3^\circ$  of the mechanical bore-sight axis, which shall be established with respect to vendor-specified datum planes.
10. No side lobe shall exceed -12 dB (one-way) with respect to the electrical beam maximum.
11. The antenna shall operate at rated power expected for SIR-B. (Note 2)
12. Other pattern requirements -- (Note 3)

Notes:

1. Vendor shall supply necessary switches and TTL-compatible logic drivers. If the switch driver is an integral part of the antenna assembly, the vendor will locate all necessary power and command connectors on the rear panel of the antenna and provide mating connectors.
2. Full power is desirable, but if this becomes too expensive, reduced power can be tolerated. However, some demonstration of power handling capability, full-power losses, etc. should be made by the vendor before final contracts are awarded.

TABLE I. (continued)

3. Horizontal plane beam width is determined from the 1.83 m (6') horizontal dimension. Vertical plane beam width will depend on the division of vertical space between frequencies, polarizations, and modules. To minimize vertical beam width, this division should be proportional to wavelength. In any event, the maximum half-power beam width of any mode-frequency-polarization combination should be held to less than  $30^\circ$  to minimize ground scatter during far-field antenna range measurements.

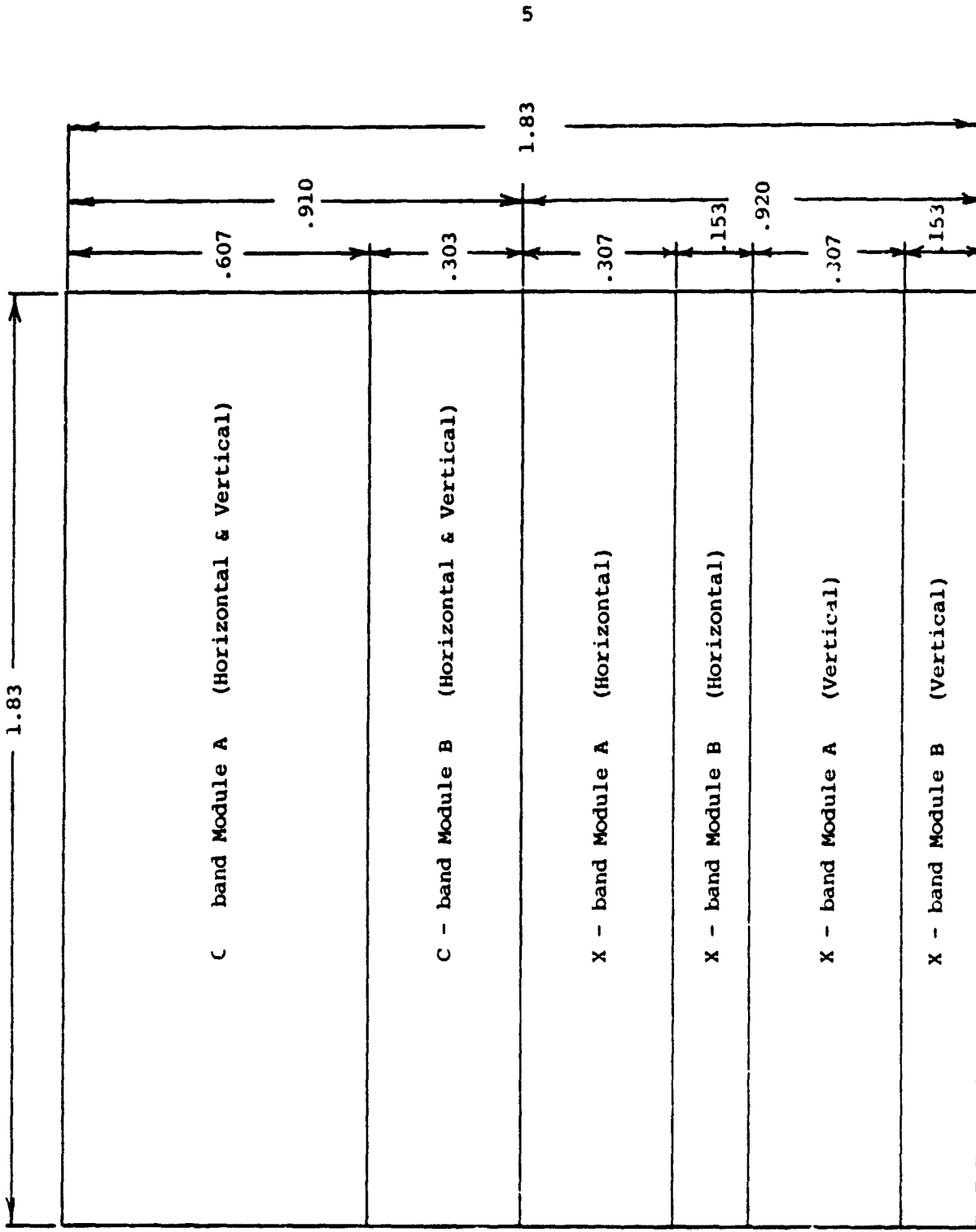


Figure 2.1. Shuttle imaging radar antenna test panel allocation of area.

TABLE II. Shuttle Imaging Radar Antenna Test Panel Mechanical Specifications

1. Dimensions of the mechanical structure shall be less than 2.13 m by 2.13 m. (7' x 7')
2. Total weight of the electrical/mechanical structure shall not exceed 90 kg. (198 lbs.)
3. Antenna should be mounted on a mechanical support, representative of space qualified designs, but full rigidity necessary in a space environment is neither required nor expected.
4. Design should recognize that mechanical testing will induce up to two cm convex and concave deflections over the length of the antenna. Maximum rate of change in deflection shall be less than 2 cm/m.
5. Rear of antenna shall be a flat metal plate, securely fastened to the electrical antenna so that when deflections are induced, the antenna deflection will replicate the plate deflection.
6. Primary support shall be a bolt circle 0.152 m in diameter centered at the center of mass of the electrical/mechanical structure.
7. An array of stress pads, spaced 0.305 m over the rear of the antenna, shall be attached to the rear plate. These should be drilled and tapped for 3/8" - 16 bolts to a depth of 1.27 cm (1/2").
8. Electrical connectors shall be located on the rear panel at convenient locations not to interfere with the bolt circle or array of stress pads. Connector types shall be Type N for the lower frequency, UG-39 waveguide interface for the higher frequency.
9. Environmental -- The structure shall return to nominal flatness after broadside exposure to wind speeds of up to 85 knots.
10. Stability of Materials -- Electrical characteristics of materials used in antenna elements and feed lines shall be stable over long periods of time with respect to mission duration and under space vacuum conditions.
11. Vendor shall propose techniques for folding mechanism for the panels and shall demonstrate that the full-sized array will perform with electrical characteristics scaled from that of the test panel. Vendor is not expected to deliver test panel with a folding mechanism but instead is required to demonstrate proof of concept.

### 2.1.1 Electrical Structure

1. "Electrical structure dimensions shall be 1.83 m x 1.83 m (6' x 6') +10%"

The electrical size of the test panel was made using the following criteria:

- 1) the area was electrically large enough to allow meaningful electrical and thermal tests which could, with a computer simulation model, be used to predict full-size array performance, and 2) the antenna effective aperture was small enough to conveniently make pattern tests using both near-field and far-field techniques.

Criterion (2) is most restrictive. The rule-of-thumb used by most antenna engineers for pattern testing is that the separation between the source and test antenna be greater than  $2D^2/\lambda$ , where D is the test antenna maximum dimension. This criterion corresponds to a  $\lambda/16$  ( $22\frac{1}{2}^\circ$ ) path length difference between the source antenna and the extreme of a test antenna. For precise measurement of null depths and side lobe levels, several times this distance may be necessary. Using four times the rule-of-thumb distance corresponds to an aperture size of 1.87 m (6.135') at X-band when being tested on the 3000' PSL range. This criterion ( $8D^2/\lambda$ ) should provide sufficient accuracy for all necessary measurements. Therefore, six feet is chosen as an upper-bound on the array dimensions.

Heavy ground scatter along the 3000' range can be avoided by using a 4' - 6' parabolic dish as the transmitting antenna. With a transmitting antenna diameter of this size, the far-field criterion becomes  $2(D_r + D_t)^2/\lambda$  where  $D_r$  is the receive antenna diameter and  $D_t$  is the transmit antenna diameter. With  $D_r = D_t = 6'$ , the 3000' range still places the receive antenna in the far field.

### 2.1.2 Frequency of Operation

2. "The antenna shall be dual frequency at 4.75 and 9.60 GHz."

At the time the test panel specifications were made, the full-size SIRA was to operate at both C- and X-band.

### 2.1.3 Polarization

3. "The antenna shall have both horizontal and vertical polarization capability at each frequency."

At the time these test panel specifications were made, the full-size SIRA was projected to operate in HH, HV, VV, VH modes.

### 2.1.4 Beam Width Switching

4. "There shall be two modules at each frequency (and/or polarization) to replicate beam width switching to be employed on the full-size SIRA."

This specification was to simulate SIRA elevation beam switching, with the first module having twice the elevation width of the second. Originally, the SIRA was to operate with a 100 km swath width over off-nadir angles of between  $7^{\circ}$  and  $50^{\circ}$ , and three selectable beam widths were necessary to maintain a constant swath width for various incidence angles. As of this writing, the multiple beam width question has not yet been decided. Therefore, it is recommended that the test panels incorporate this feature.

### 2.1.5 Antenna Gain

5. "The antenna gain using both modules shall be at least 32 dB at 4.75 GHz and 33 dB at 9.6 GHz. Antenna gain shall be optimized within the bounds of other specifications."

If the C-band H and V elements can share the same physical aperture, then, assuming an aperture efficiency of 55%, a gain of 34.6 dB is theoretically possible. Assuming 2.6 dB for feedline and connector losses gives the specified gain of 32 dB. At X-band a theoretical gain of 37.7 dB is possible. The 33 dB figure specified allows for 4.7 dB in losses. Both Hughes and JPL/Ball Bros. have estimated losses on the order of 2.6 dB at C-band and 3.7 dB at X-band. Hence, the numbers specified are conservative. However, it is more important (at least for the test panels) to meet all specifications than to require an unobtainable antenna gain.

### 2.1.6 Antenna Insertion Loss

6. "The total antenna loss (ratio of maximum gain to maximum directivity) shall not exceed 1.5 dB."

The noise power generated by the loss in the antenna degrades the system noise temperature by

$$\begin{aligned} T_{\text{sys}} &= \frac{T_a}{L} + T_o \left(1 - \frac{1}{L}\right) + T_o (F_r - 1) \\ &= \left(F_r - \frac{1}{L}\right) T_o \end{aligned} \quad (2-1)$$

where  $T_{\text{sys}}$  = System noise temperature

$T_a$  = Antenna integrated incident brightness temperature  
( $T_a \approx 0$ )

$L$  = Antenna loss (power ratio)

$F_r$  = Noise figure of receiver (power ratio)

$T_r$  = Receiver noise temperature =  $T_o (F_r - 1)$

$T_o$  = 290K (standard; assumed the same for antenna structure and receiver box)

Preliminary estimates by Hughes and JPL have indicated that a receiver with a noise figure of 2.5 dB ( $F_r = 1.778$ ) will be required to obtain a satisfactory signal-to-noise ratio (SNR). From equation (2-1), a 1.5 dB insertion loss ( $L = 1.4125$ ) degrades the system noise temperature to 438 K, versus 226 K for the lossless case. The signal-to-noise ratio under these circumstances will be degraded by

$$\begin{aligned}\text{SNR degradation} &= 10 \log(T_{\text{sys}}/T_r) \\ &= 2.9 \text{ dB}\end{aligned}$$

(Conversely, to maintain a system noise figure of 2.5 dB with an antenna insertion loss of 1.5 dB requires that the receiver noise figure be better than 1.0 dB.)

While exact figures are not available, certainly no more than a 2.9 dB SNR degradation would be acceptable, thus leading to the 1.5 dB antenna loss constraint.

#### 2.1.7 Antenna VSWR

7. "The V. SWR in any mode of operation shall not exceed 1.3:1."

A VSWR of 1.3 should be readily obtained over a 35 MHz bandwidth. This corresponds to a mismatch loss of less than 0.1 dB.

### 2.1.8 Polarization Purity

8. "For any mode of operation, the cross-polarized component shall be at least -30 dB with respect to the maximum principal polarization component as measured over the entire beam."

Both Hughes and JPL/Ball Bros. have specified a -30 dB cross-polarization level. While there is doubt as to whether or not this level can be maintained in a space environment (with thermal and mechanical distortions induced on the antenna surface), undistorted cross-polarization level should be as low as possible on the test panels so that when the panels are artificially distorted, an accurate measurement of the cross-polarization degradation can be made and entered into the computer simulation model. It should also be pointed out that a measurement of this level cross-polarized energy will be difficult.

### 2.1.9 Beam Pointing Accuracy

9. "The electrical beam maximum shall be within  $0.3^\circ$  of the mechanical boresight axis, which shall be established with respect to vendor-specified datum planes."

The 3-dB azimuth beamwidth (at C-band) for the full-size SIRA is  $0.34^\circ$ . While it may not be necessary to maintain a  $0.3^\circ$  beam pointing accuracy for the test panels (except to facilitate measurements), it certainly will be necessary to maintain better than  $0.3^\circ$  accuracy for the full-size array. (At an altitude of 200 km, an error of  $0.3^\circ$  corresponds to 1.05 km on the earth's surface.) In addition, measurements of beam position versus test panel distortion will be much easier and much more accurate with a beam aligned with mechanical boresight.

#### 2.1.10 Side Lobe Level

10. "No side lobe shall exceed -12 dB (one-way) with respect to the electrical beam maximum."

To obtain three easily switched beam widths on the SIRA, uniform illumination of each module is required (as indicated by both JPL/BBRC and Hughes). The theoretical side lobe level (SLL) for a uniformly illuminated aperture is -13.2 dB. A reasonable SLL for an antenna the size of the test panels is on the order of 0.7 to 1.0 dB worse.

#### 2.1.11 Power Handling Requirements

11. "The antenna shall operate at rated power expected for SIR-B."

Up to this point in time, no demonstration of power handling capability has been made by any potential vendor. While full power is desirable for the test panels, it certainly is not necessary for the measurements that will be made using them. However, some demonstration of power handling capability, full power losses, etc. should be made before final SIRA contracts are awarded. As an example, the peak power contemplated for SIR-A is approximately 1800 W.

#### 2.1.12 Other Pattern Requirements (Note 4, Table I)

A maximum half-power beamwidth of  $30^\circ$  is necessary to minimize ground scatter during far-field antenna measurements. Horizontal beam width is determined from the 1.83 m (6') horizontal dimension and corresponds to  $1.8^\circ$  at C-band and  $1.2^\circ$  at X-band. Vertical beam widths depend on the division of vertical space between frequencies, polarizations, and modules. If horizontal and vertical C-band elements can be shared, and if separate X-band elements

are used, then a division of space as shown in Figure 2.1 will give minimum vertical beamwidth, which is  $1.06^\circ$  with module B at either frequency.

## 2.2 Mechanical Specifications

### 2.2.1 Mechanical Dimensions

1. "Dimensions of the mechanical structure shall be less than 2.13 m by 2.13 m (7' x 7')."

Since the electrical structure is constrained to 6' x 6', a mechanical structure of 7' x 7' should be sufficient. A larger structure would pose unnecessary problems in mounting/demounting.

### 2.2.2 Weight

2. "Total weight of the electrical/mechanical structure shall not exceed 90 kg."

The weight is constrained by the positioner weight/bending moment specifications plus expected weight/size of the mechanical deformation simulator.

### 2.2.3 Support Structure

3. "Antenna should be mounted on a representative mechanical support, but full rigidity necessary in a space environment is neither required nor expected."

One of the goals of the deformation tests is to determine the rigidity necessary to properly support the antenna under expected in situ mechanical/thermal conditions. Hence, time and money expended in a back-up structure at this point may be unnecessarily wasted. Furthermore, the antenna will be

artificially deformed up to two cm from nominal flatness, and a too-rigid structure will hinder these deformation tests.

#### 2.2.4 Mechanical Deformation Testing

4. "Design should recognize that mechanical testing will induce up to two cm convex and/or concave deflections over the area of the antenna. Maximum rate of change in deflection shall be less than two cm/m."

Preliminary computer simulations show that five cm distortions on the full-size antenna at C- or X-band degrade the antenna footprint to a point where it is no longer usable in a synthetic aperture radar system. For example, at X-band, a five cm parabolic bow (simulating uneven heating) degrades antenna gain by as much as 10 dB, while a panel unfolding error of -1cm/2cm gives a degradation of 3 dB.

For the smaller test panels, a two cm maximum bow should be sufficient to demonstrate deformation effects on the antenna pattern.

#### 2.2.5 Interface with PSL Deformation Simulator

5. "Rear of antenna shall be a flat metal plate, securely fastened to the electrical antenna so that when deflections are induced, the antenna deflection will replicate the plate deflection."

6. "Primary support shall be a bolt circle 0.152 m in diameter centered at the center of mass of the electrical/mechanical structure."

7. "An array of stress pads, spaced 0.305 m over the rear of the antenna, shall be attached to the rear plate. These should be drilled and tapped for 3/8" - 16 bolts to a depth of 1.27 cm (1/2")."

The weight-bearing point will be the 0.152 m (6") bolt circle centered at the structure's center of mass. Deformation from flatness will be induced by

adjusting lead screw depth at each stress pad. The antenna deflection should replicate this deformation.

#### 2.2.6 Connectors

8. "Electrical connectors shall be located on the rear panel at convenient locations not to interfere with the bolt circle or array of stress pads. Connectors shall be Type N for the lower frequency, UG-39 waveguide interface for the higher frequency."

#### 2.2.7 Environmental and Stability of Materials

9. "Environmental -- The structure shall return to nominal flatness after broadside exposure to wind speeds of up to 85 knots.

10. Stability of Materials -- Electrical characteristics of materials used in antenna elements and feed lines shall be stable over long periods of time under space vacuum conditions."

#### 2.2.8 Folding Mechanism

11. "Vendor shall propose technique for folding mechanism for the panels and shall demonstrate that the full-sized array will perform with electrical characteristics scaled from that of the test panel. Vendor is not expected to deliver test panel with a folding mechanism but instead is required to demonstrate proof of concept."

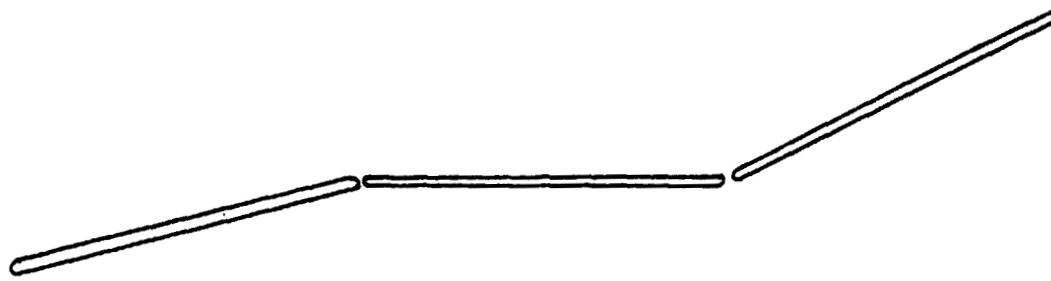
### 3.0 COMPUTER SIMULATION OF MECHANICAL/THERMAL DEFORMATIONS

Since the mathematical model of and the computer program for antenna simulations were developed and tested during Phase I, it has been possible to begin the simulation of various scenarios in Phase II. The purpose of the Phase II simulations was to gain insight into the effect of surface flatness errors on

1. Beam pointing error
2. Gain degradation
3. Main beam spreading and break-up
4. Side lobe level degradation

Simulations of two types of errors, namely panel unfolding errors and parabolic errors created by thermal gradients through the antenna (as shown in Figure 3.1), were performed at 1.5, 4.5, 9.0, 12.0, and 14.0 GHz. Footprint contour maps of fifteen representative simulations are shown in section 4.0. As would be expected, the effect of errors on antenna parameter degradation were more severe at higher frequencies.

In all cases an 11.6 m antenna azimuth length was used, as well as a 200 km altitude. Elevation length was fixed at  $8 \frac{1}{2}$  wavelengths to give a constant elevation beam width of six degrees. It was unnecessary to vary the elevation pattern for the simulations shown in Figure 3.1, since each simulation affected only the azimuth pattern. Two off-nadir angles (10 and 50 degrees) were simulated to show the interaction of this parameter with flatness errors and frequency.



(a) Panel unfolding error



(b) Parabolic bow simulating thermal distortion

Figure 3.1. Antenna deformation configurations used in the computer model.

### 3.1 Effects of Errors On Antenna Gain

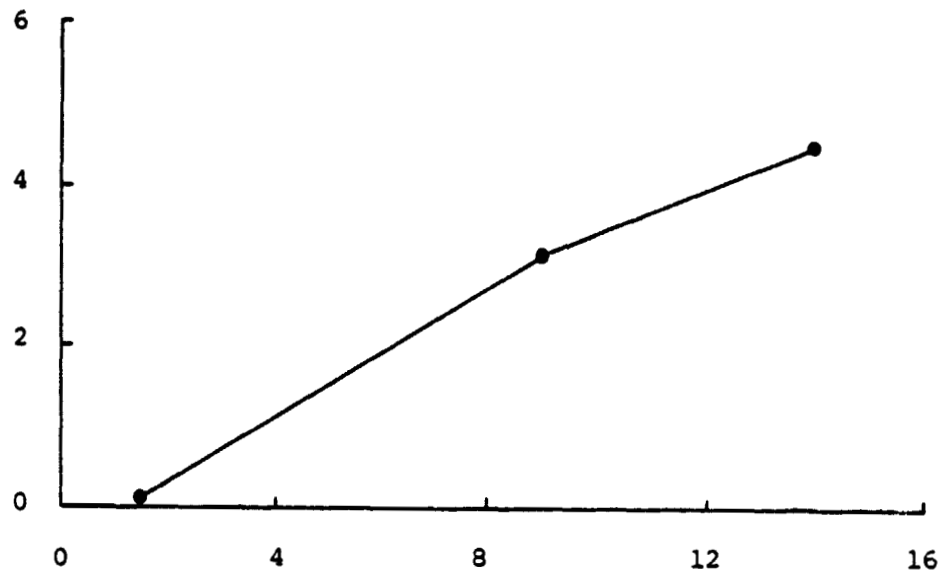
Static gain errors will affect the system signal-to-noise ratio (SNR). Furthermore, slow changes in the antenna gain over a period of hours or days cause instability in the system calibration.

Figures 3.2, 3.3, 3.4, and 3.5 illustrate the degradation of beam antenna gain from panel unfolding errors and parabolic bow errors as both frequency and severity of warp.\* Since beam pointing errors occurred simultaneously, it was necessary to first search the footprint for maximum gain and then use this gain figure. In addition, each gain was normalized to its baseline, since the actual gain of the antenna changes at different frequencies. Also, this is a convenient way to take all losses into account, since losses should be constant with respect to panel deformation.

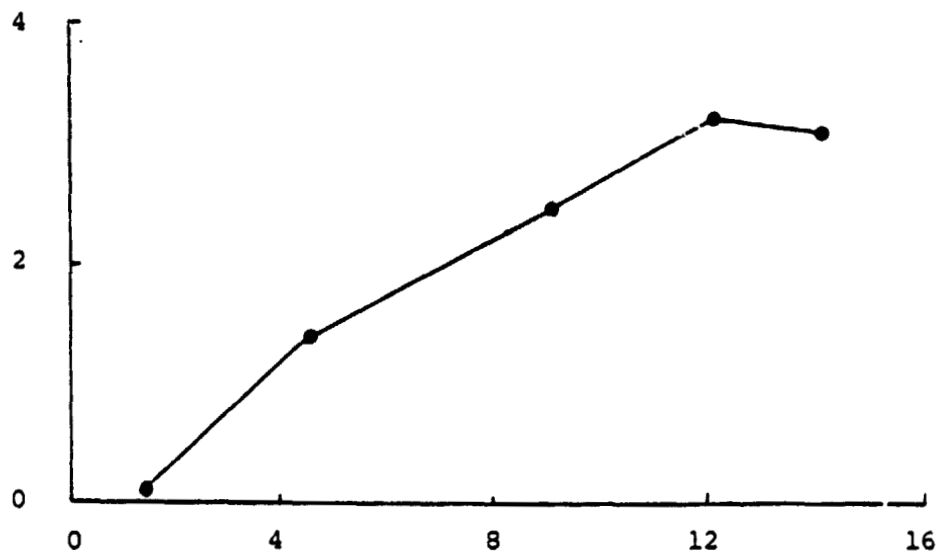
An unexpected result of the gain degradation simulation was the non-monotonic behavior of the curves. There were two contributing factors: (1) the panel degradations tended to focus the beam for certain warp errors and unfocus the beam for other errors (a resonance phenomenon), and (2) the gain search mentioned above did not find the true maximum gain because of discretization of the footprint pattern into a finite number of sample points. To determine which of these two factors is primarily responsible for the curve

---

\* Refer to the legend sketches on the contour maps of Section 4 for an explanation of the surface error convention used.

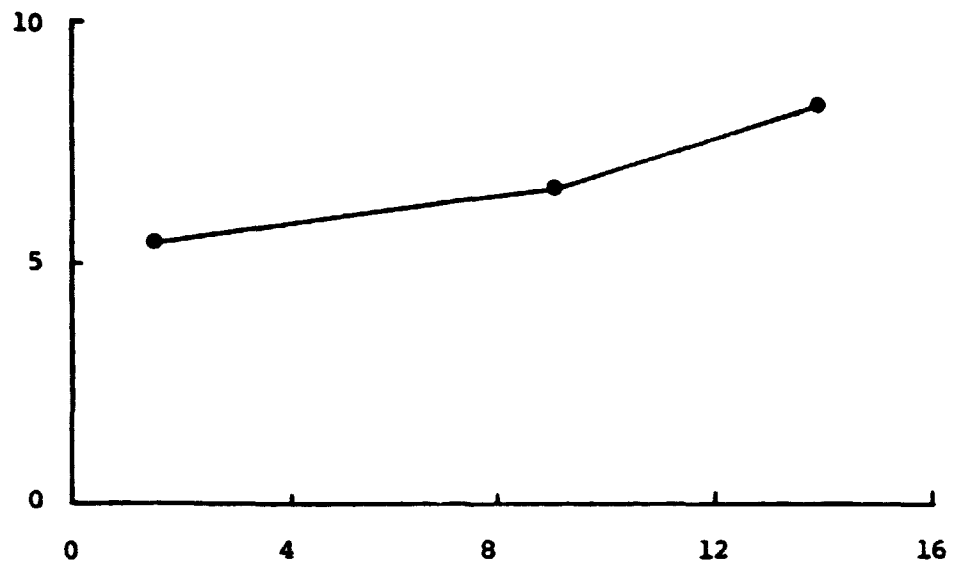


(a)

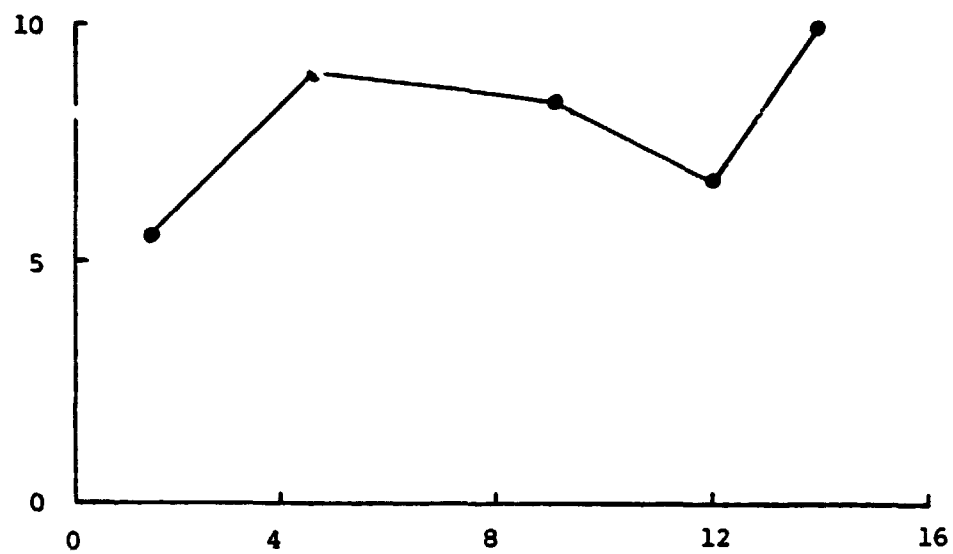


(b)

Figure 3.2. Gain degradation (dB) versus frequency (GHz) for a panel unfolding error of (-1.0, 2.0) cm at (a) 10 degree tilt (b) 50 degree tilt.



(a)



(b)

Figure 3.3. Gain degradation (dB) versus frequency (GHz) for a five cm parabolic bow at (a) 10 degree tilt (b) 50 degree tilt.

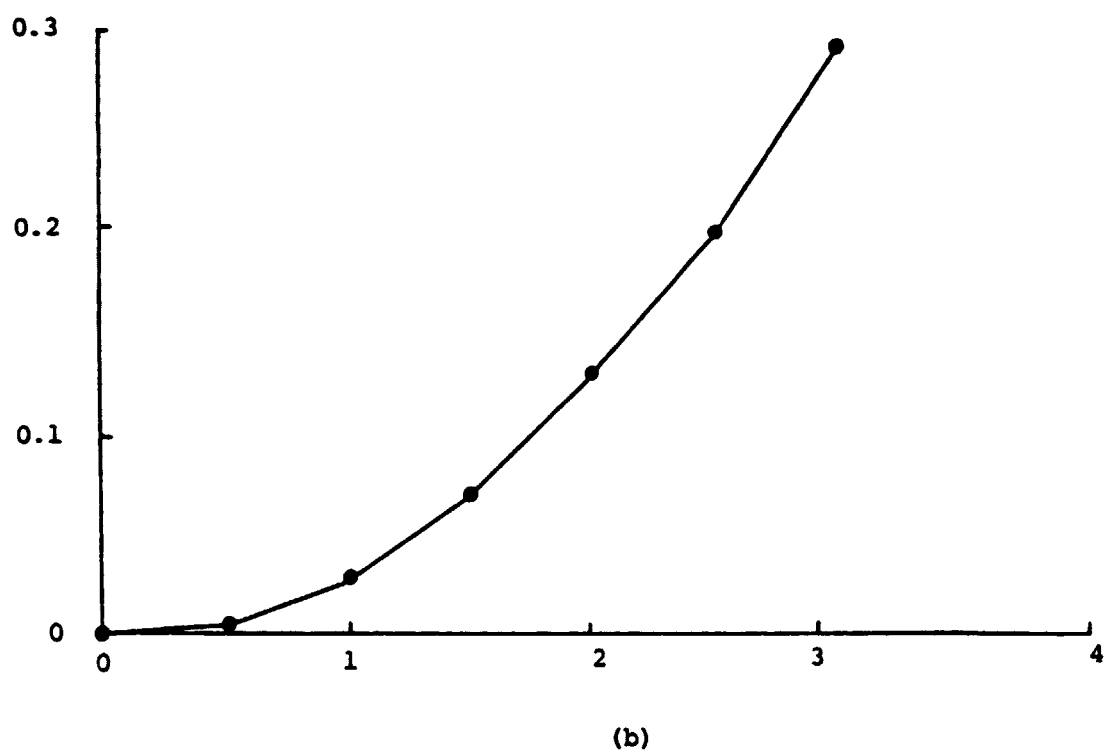
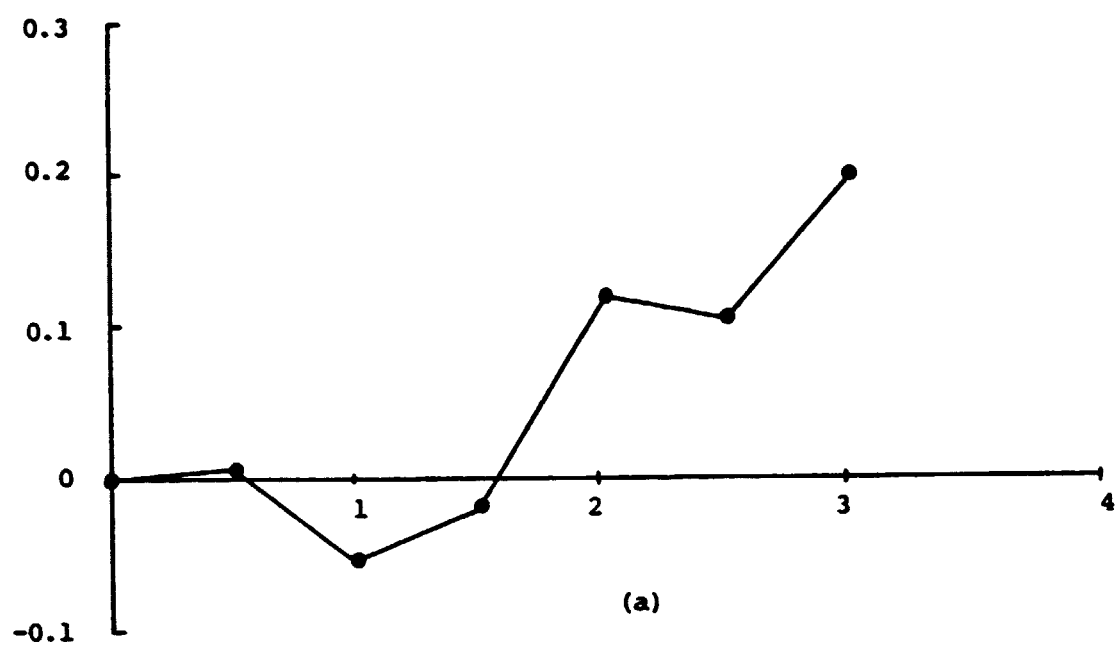
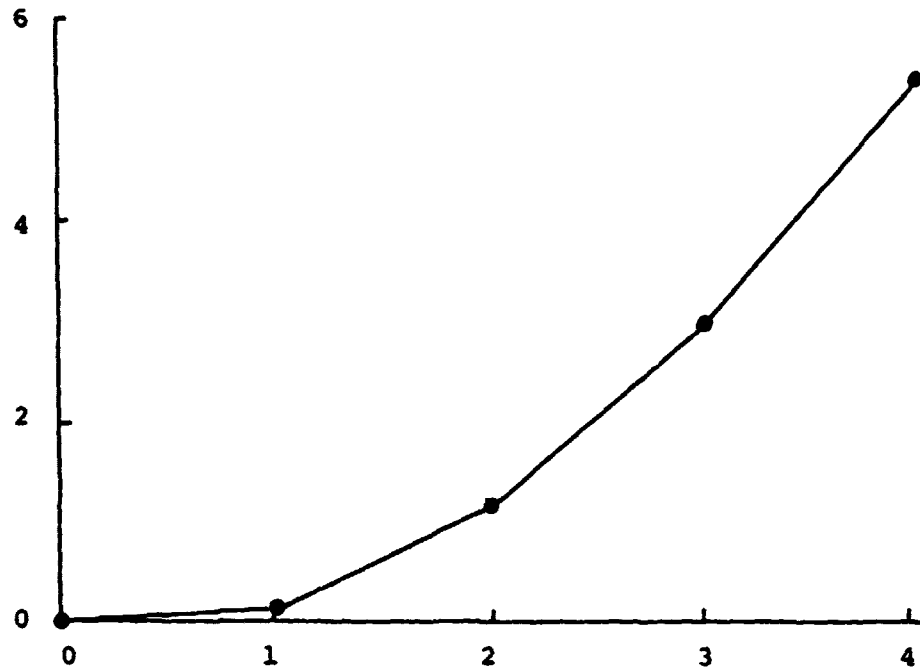
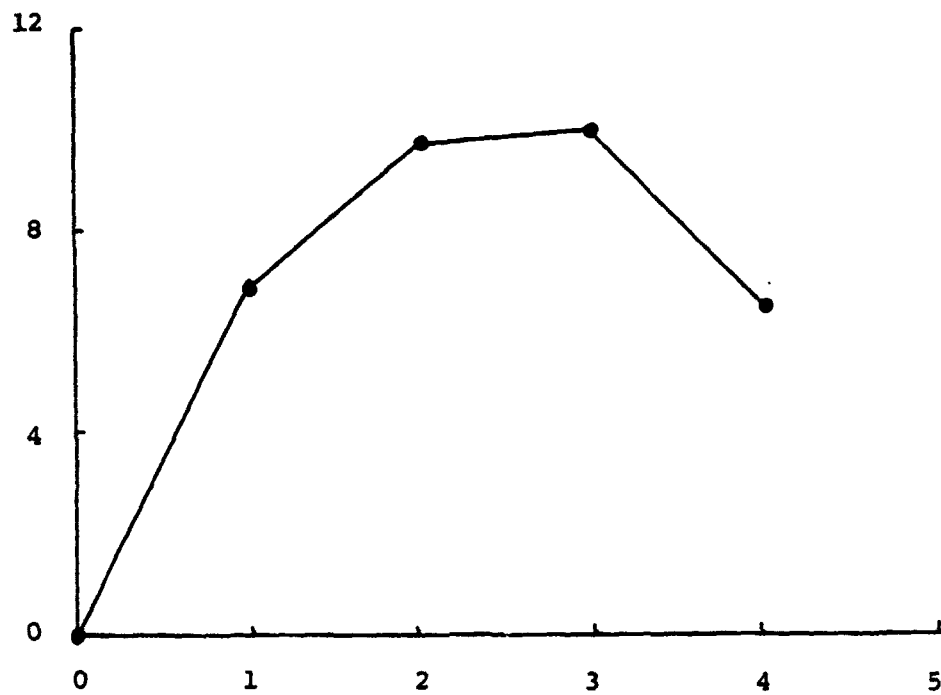


Figure 3.4. Gain degradation (dB) versus warp severity at 1.5 HGz and  $10^\circ$  tilt for (a) panel unfolding errors, (b) parabolic bow errors.



(a)



(b)

Figure 3.5. Gain degradation (dB) versus warp severity (cm) for parabolic bow errors at  $10^\circ$  tilt: (a) 1.5 GHz, (b) 9.0 GHz.

shape, it will be necessary in Phase III to perform additional simulations at intermediate data points.

### 3.2 Beam Pointing Errors

In the process of forming the synthetic aperture, it is necessary to sense any changes in the position of the antenna beam relative to the isodops (surfaces of constant Doppler frequency) so that the resulting image may be compensated. One way of doing this is to monitor in real time the average Doppler shift of the radar data, and use this information to keep the beam centered about the required isodop. A second approach would be to monitor the data and dynamically adjust the processor to compensate for deviations in beam position (as well as orbit eccentricity and angular velocity of the spacecraft). Using this approach, the antenna requirements are reduced (at the expense of increased processor complexity) to placing limits on the beam pointing error.

Figures 3.6 and 3.7 depict the beam pointing error at 1.5 and 9.0 GHz for panel unfolding errors. It was found that, for this error type, the beam pointing error was independent of frequency. There is no beam pointing error for the parabolic bow, since it is a symmetric error.

Figures 3.8 - 3.14 show the actual azimuth far-field patterns for different warp severities.

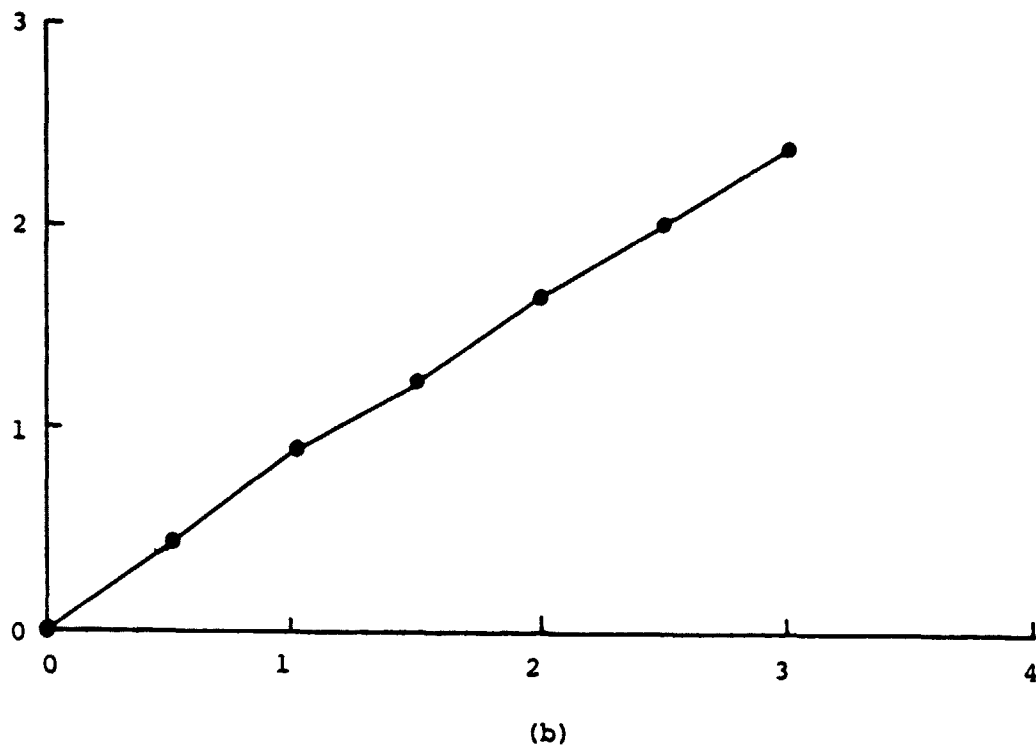
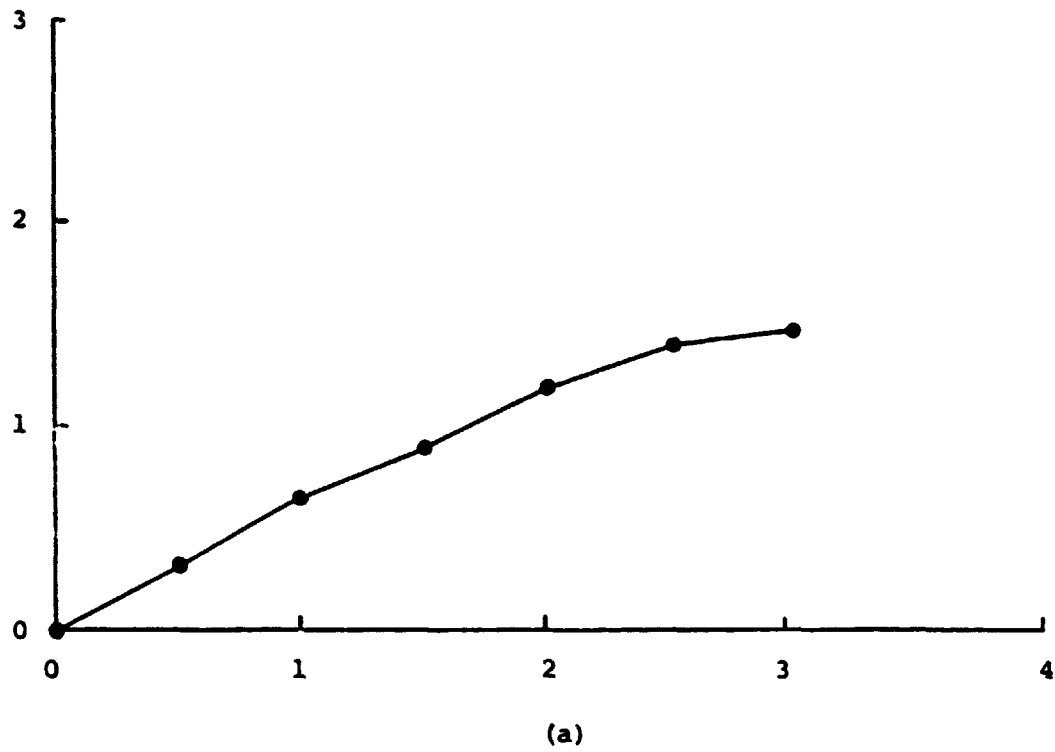


Figure 3.6. Beam pointing error (km) versus panel unfolding error (cm) at  $f = 1.5$  GHz for (a)  $10^\circ$  tilt, (b)  $50^\circ$  tilt.

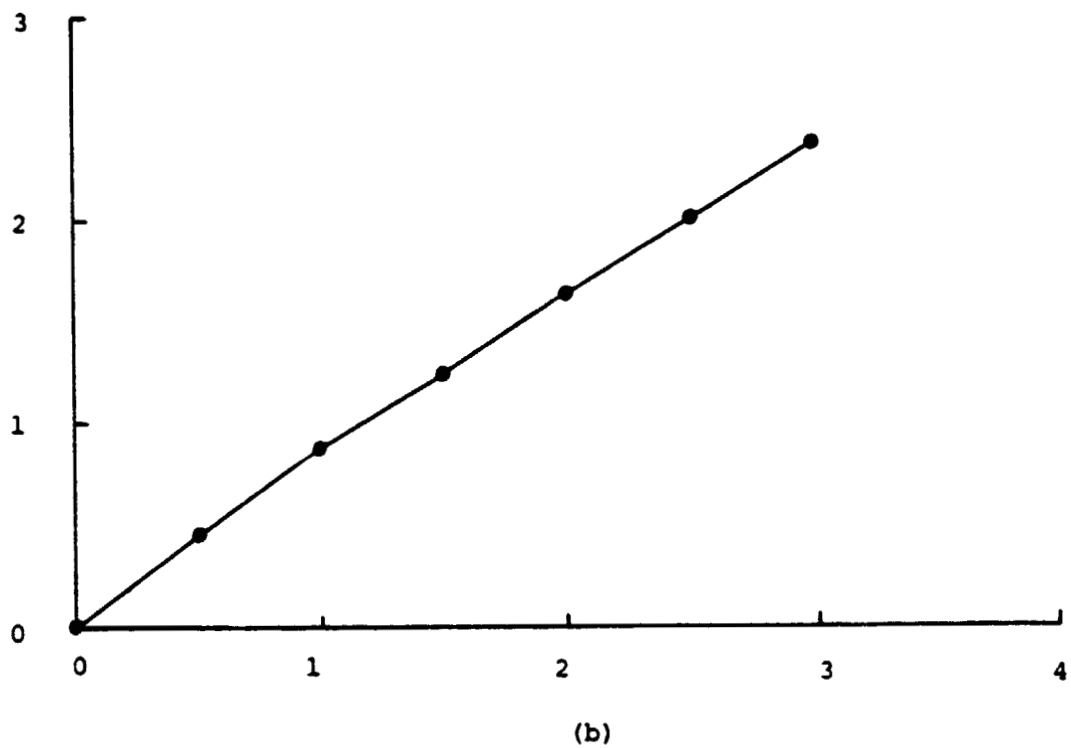
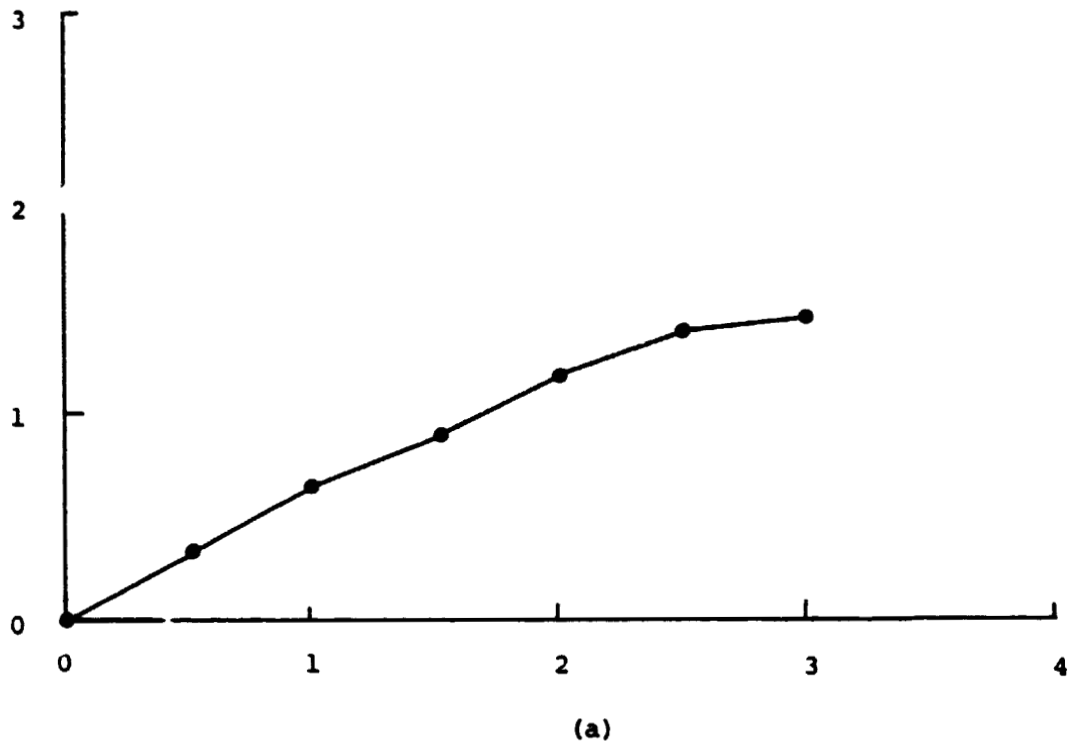


Figure 3.7. Beam pointing error (km) versus panel unfolding error (cm) at  $f = 9.0$  GHz for (a)  $10^\circ$  tilt, (b)  $50^\circ$  tilt.

# FILE 9

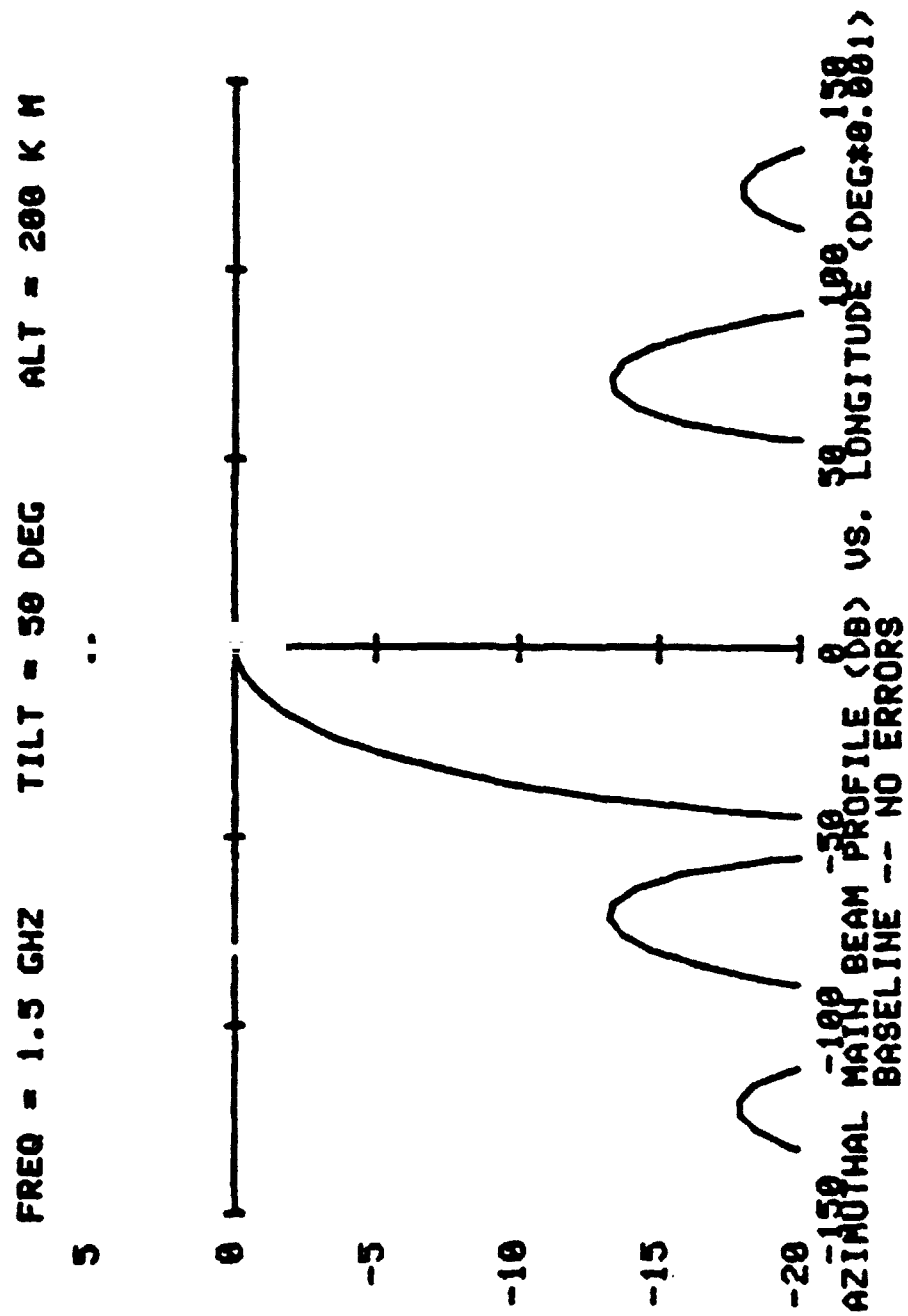


Figure 3.8 Azimuthal main beam footprint profile.

# FILE 6

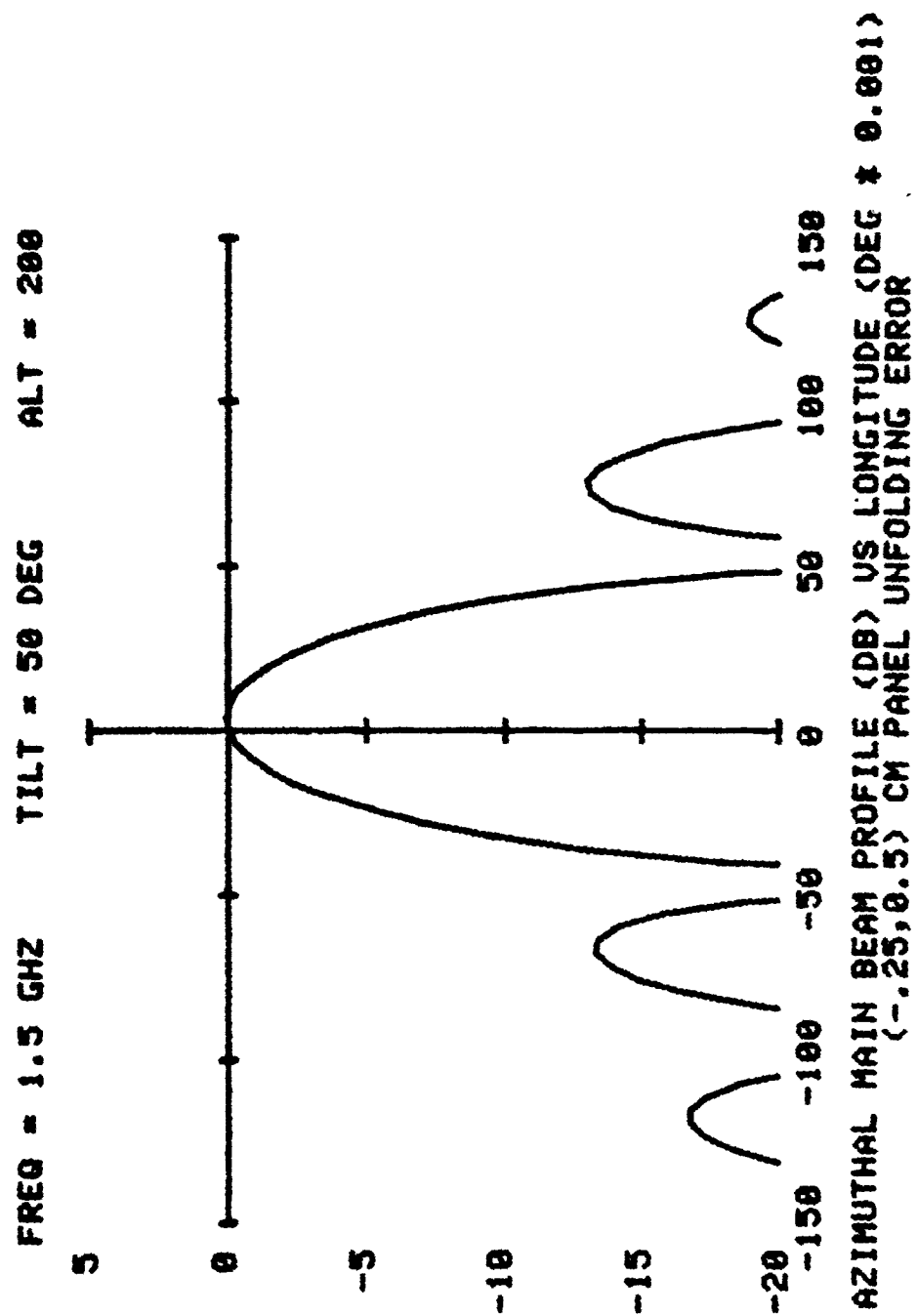


Figure 3.9 Azimuthal main beam footprint profile.

# FILE 7

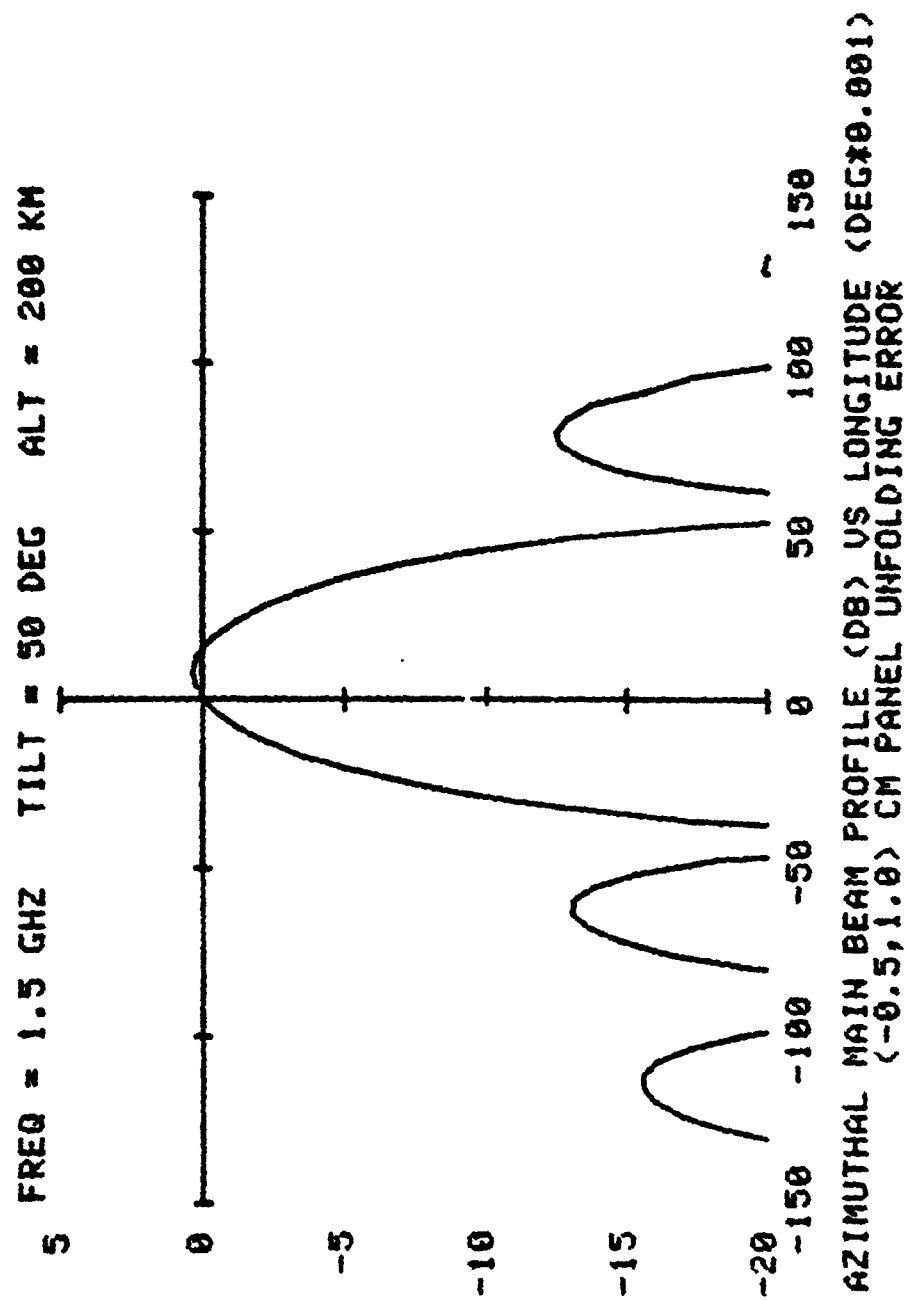


Figure 3.10 Azimuthal main beam footprint profile.

# FILE 8

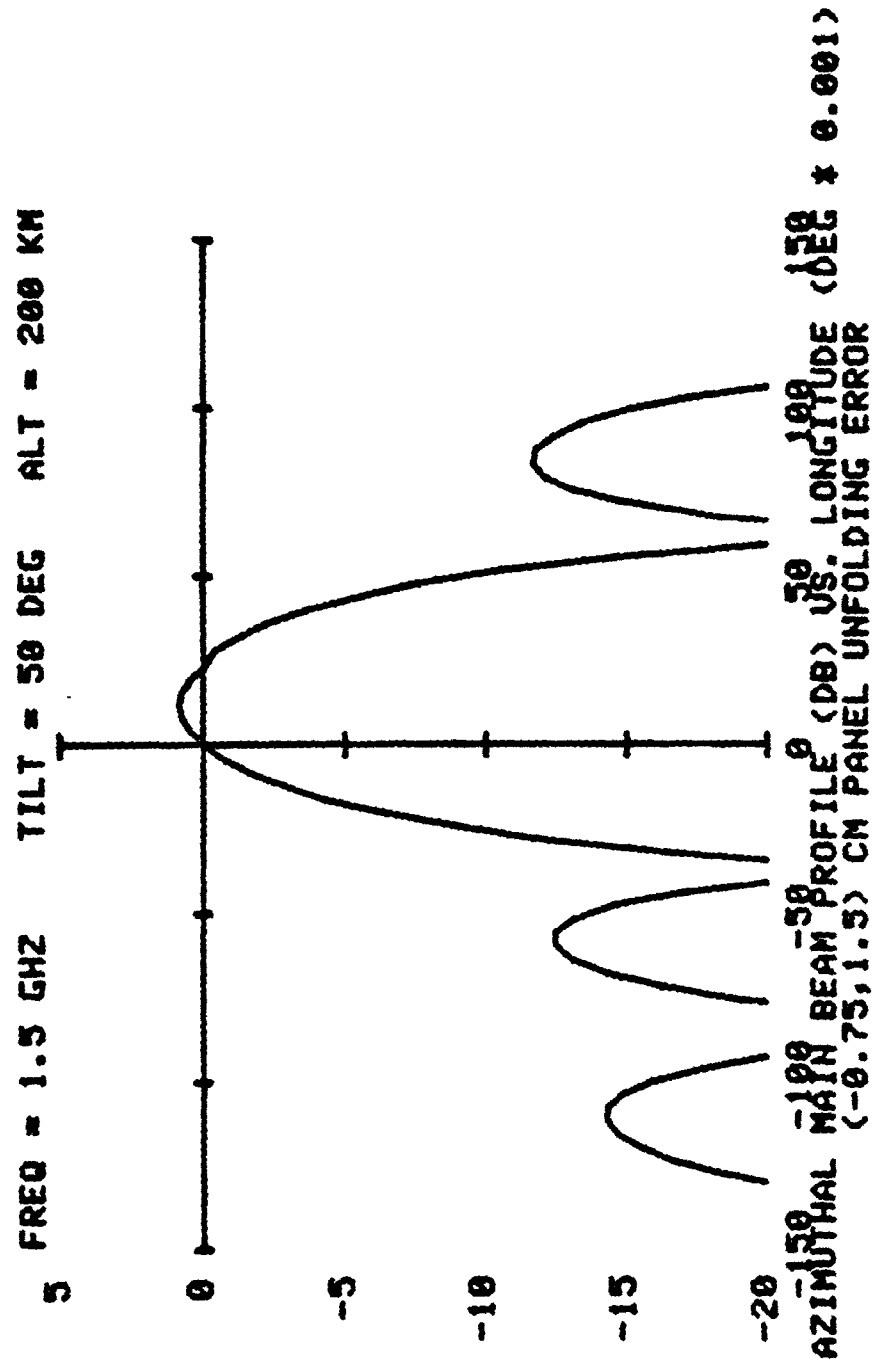


Figure 3.11 Azimuthal main beam footprint profile.

# FILE 10

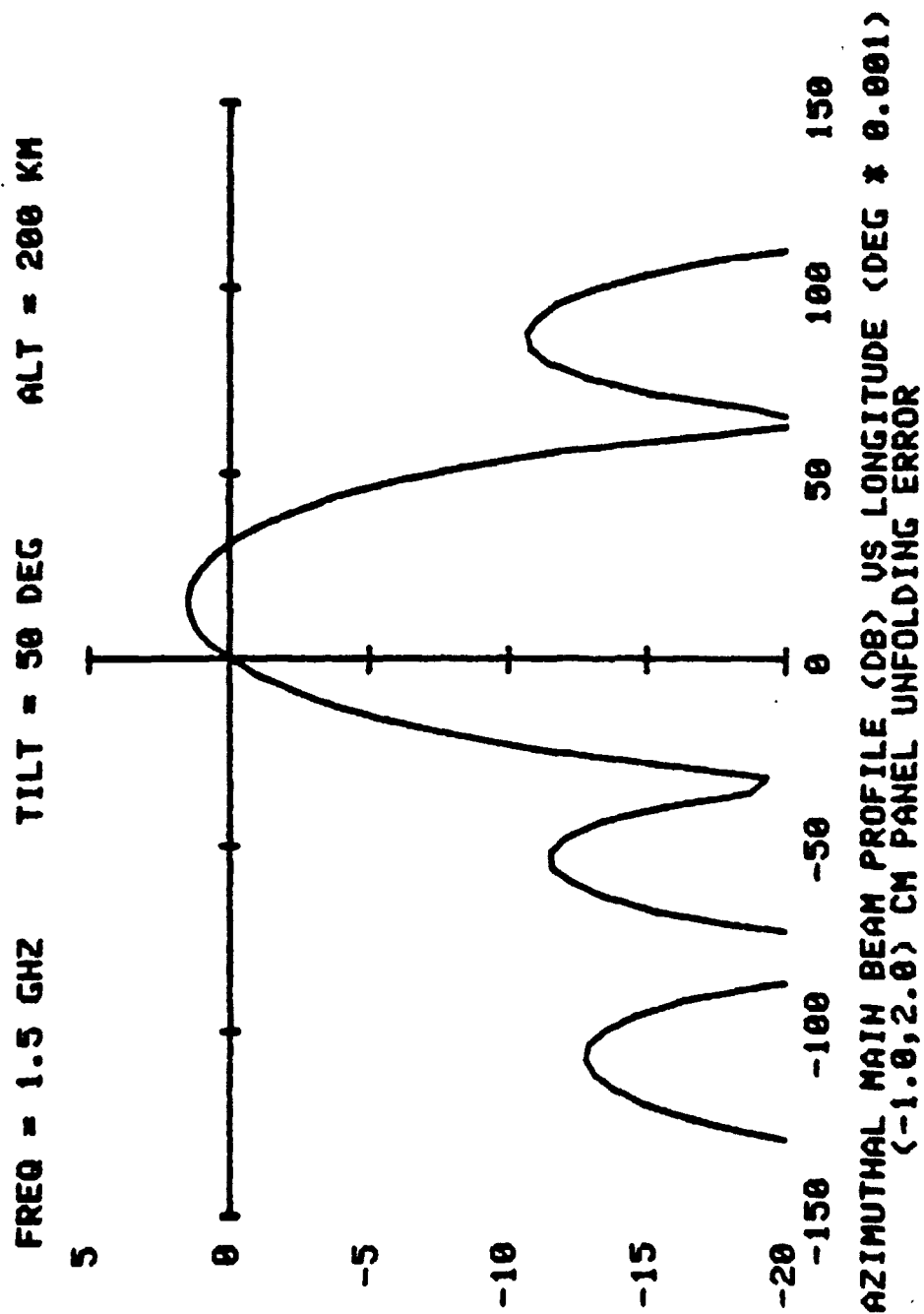


Figure 3.12 Azimuthal main beam footprint profile.

# FILE 11

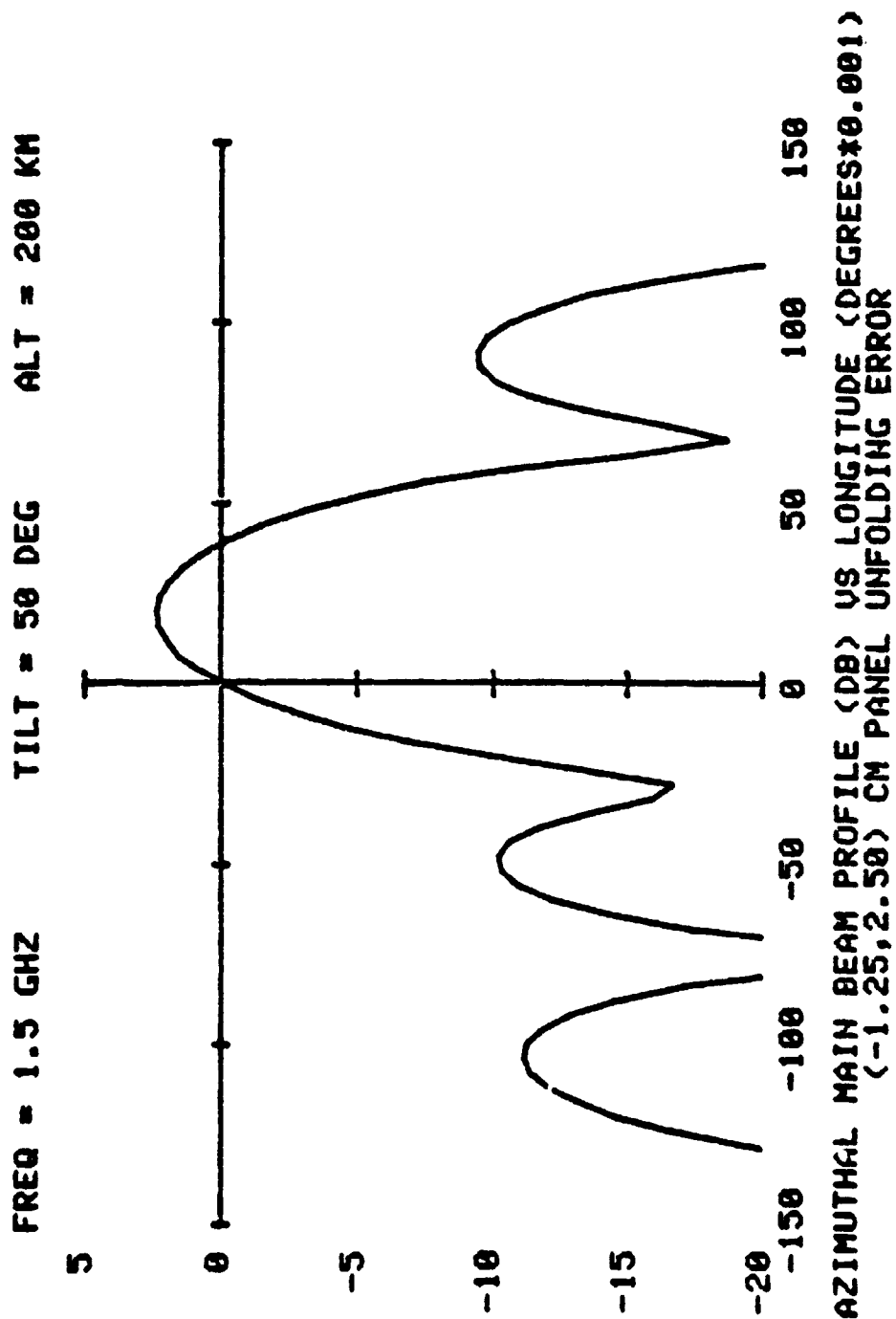


Figure 3.13 Azimuthal main beam footprint profile.

FILE 12

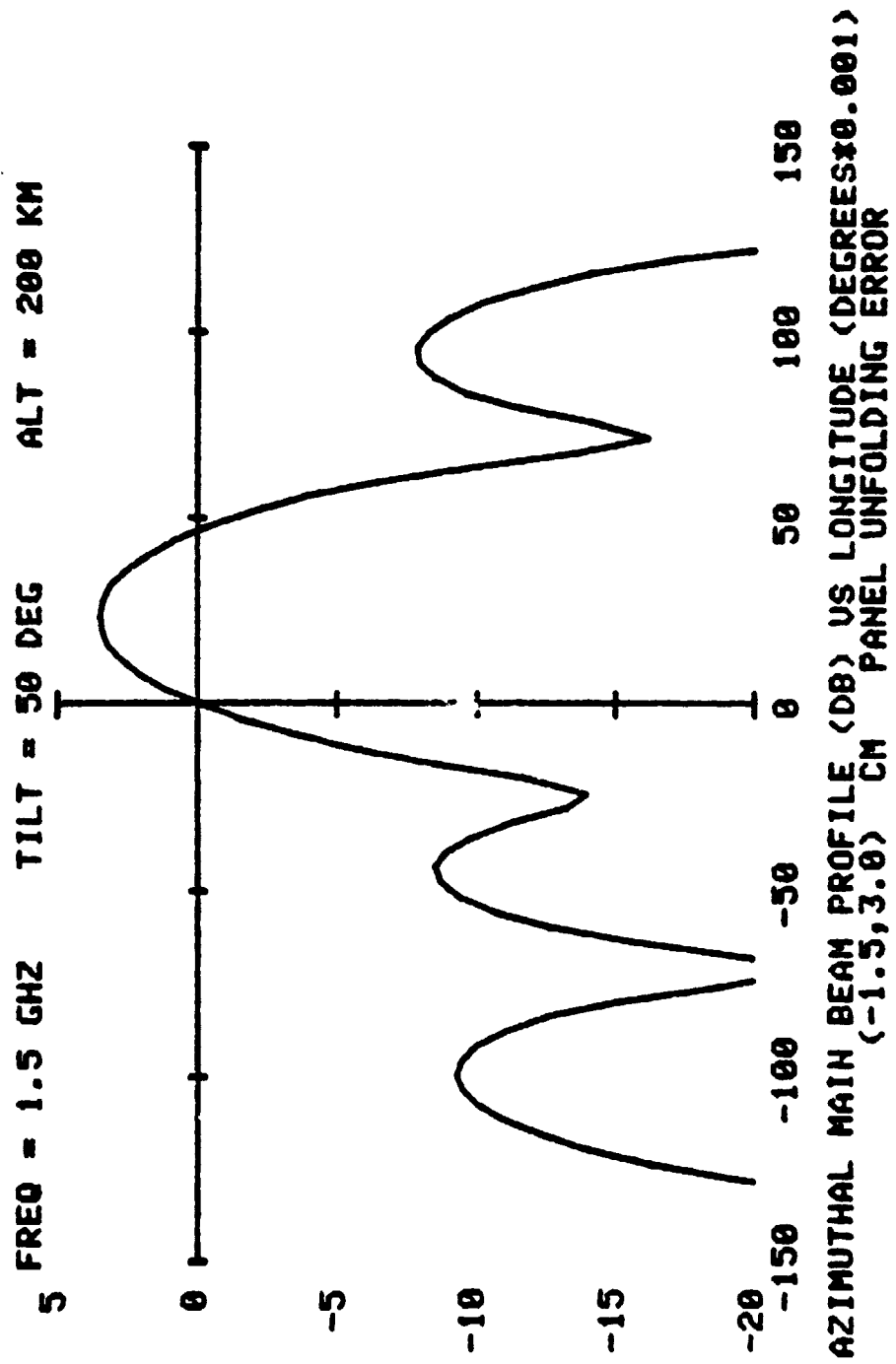


Figure 3.14 Azimuthal main beam footprint profile.

### 3.3 Main Beam Shape

The main beam shape modulates the amplitude of the data. If the beam shape is known before launch, the processor can be designed to compensate for it. If the beam shape changes during a mission, the data will be degraded.

Figures 3.15 and 3.16 summarize the effect of panel unfolding errors and parabolic bow errors on main beam spreading. The most dramatic change is in the beam area covered by the parabolic bow error. Figures 3.17, 3.18, 3.19, and 3.20 depict the azimuth footprint pattern for parabolic bow errors of 1, 2, 3, and 4 cm respectively.

### 3.4 Side Lobe Level

The principal impact of the antenna side lobe level (SLL) on the overall system is one of ambiguities within the processed image. Any rise in the side lobe level will decrease the imaged signal-to-ambiguity ratio. Furthermore, an increase in the SLL indicates that the antenna gain has decreased, degrading the SNR as well.

Another quality criterion is that of total peak to total side lobe power ratio. Even though all side lobes may fall below some relative level (for example, -20 dB), the integrated SLL power level may completely mask the presence of a fairly strong point target.

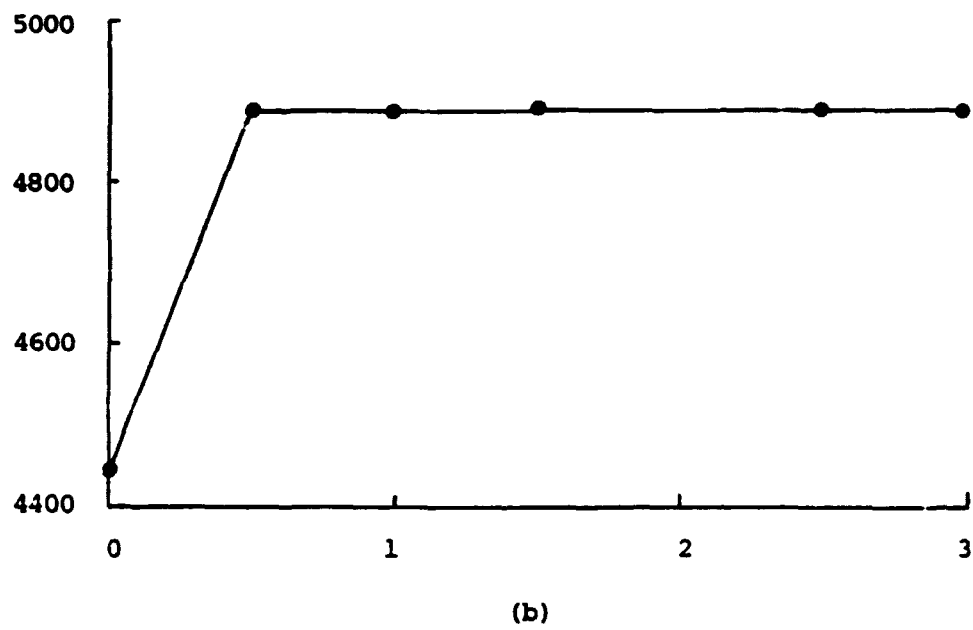
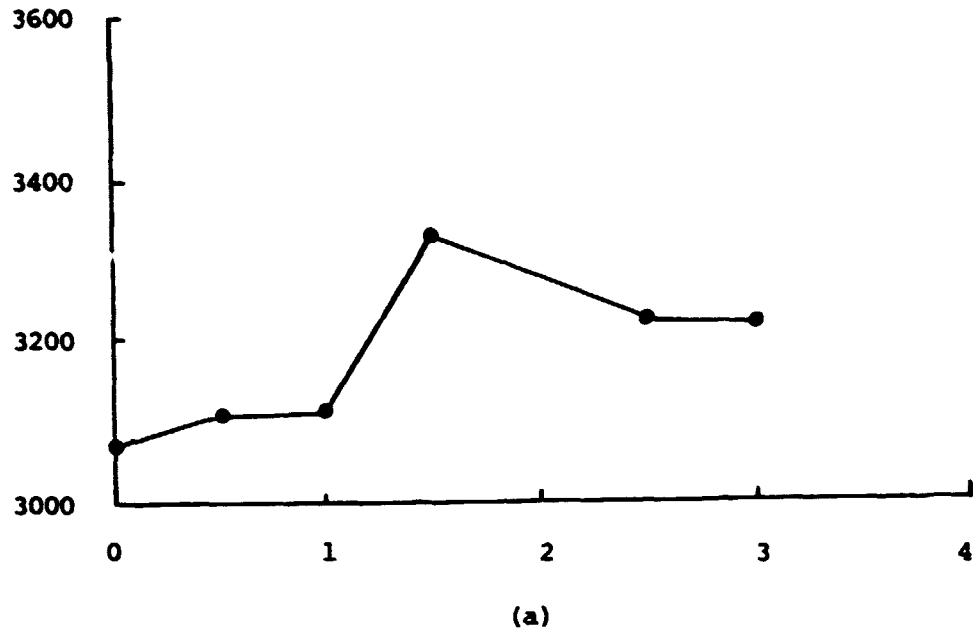


Figure 3.15. Azimuth beam width (meters) versus warp severity (cm) for panel unfolding errors at 1.5 GHz and 200 km: (a)  $10^\circ$  tilt, (b)  $50^\circ$  tilt.

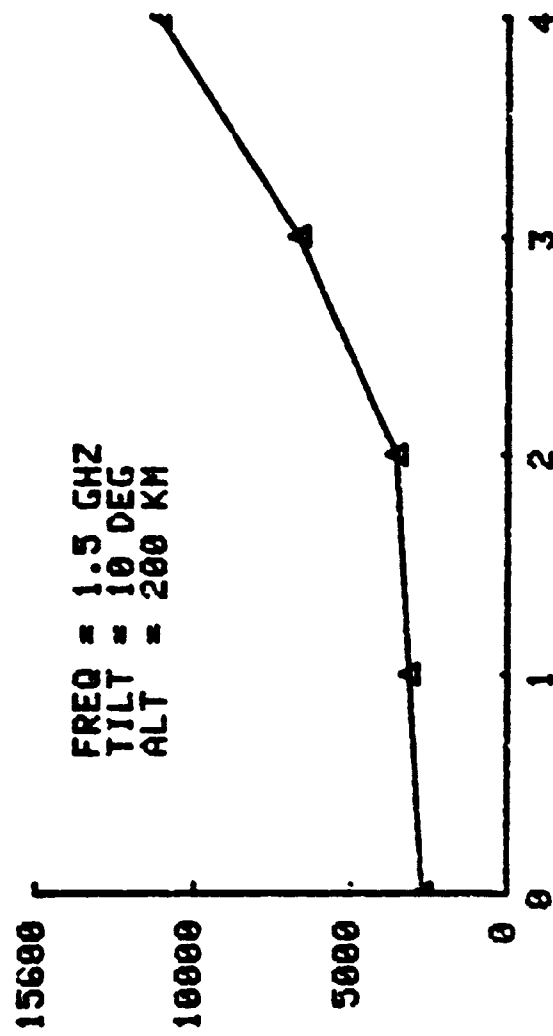


Figure 3.16 Three DB azimuth beam width (meters) vs warp severity (CM) parabolic bow error.

F = 1.5 GHZ      TILT = 10 DEG      ALT = 200 KM

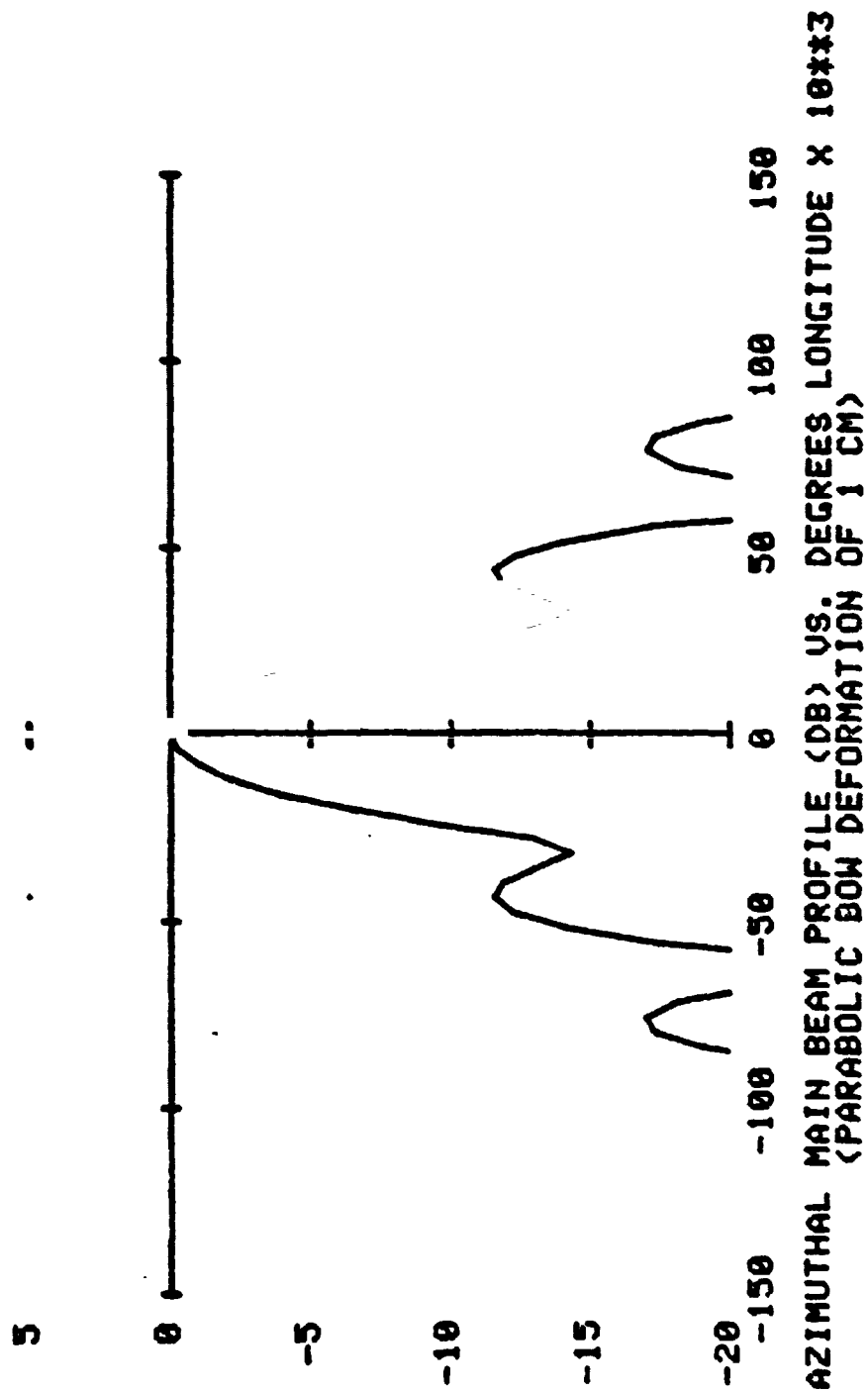


Figure 3.17 Azimuth main beam footprint profile.

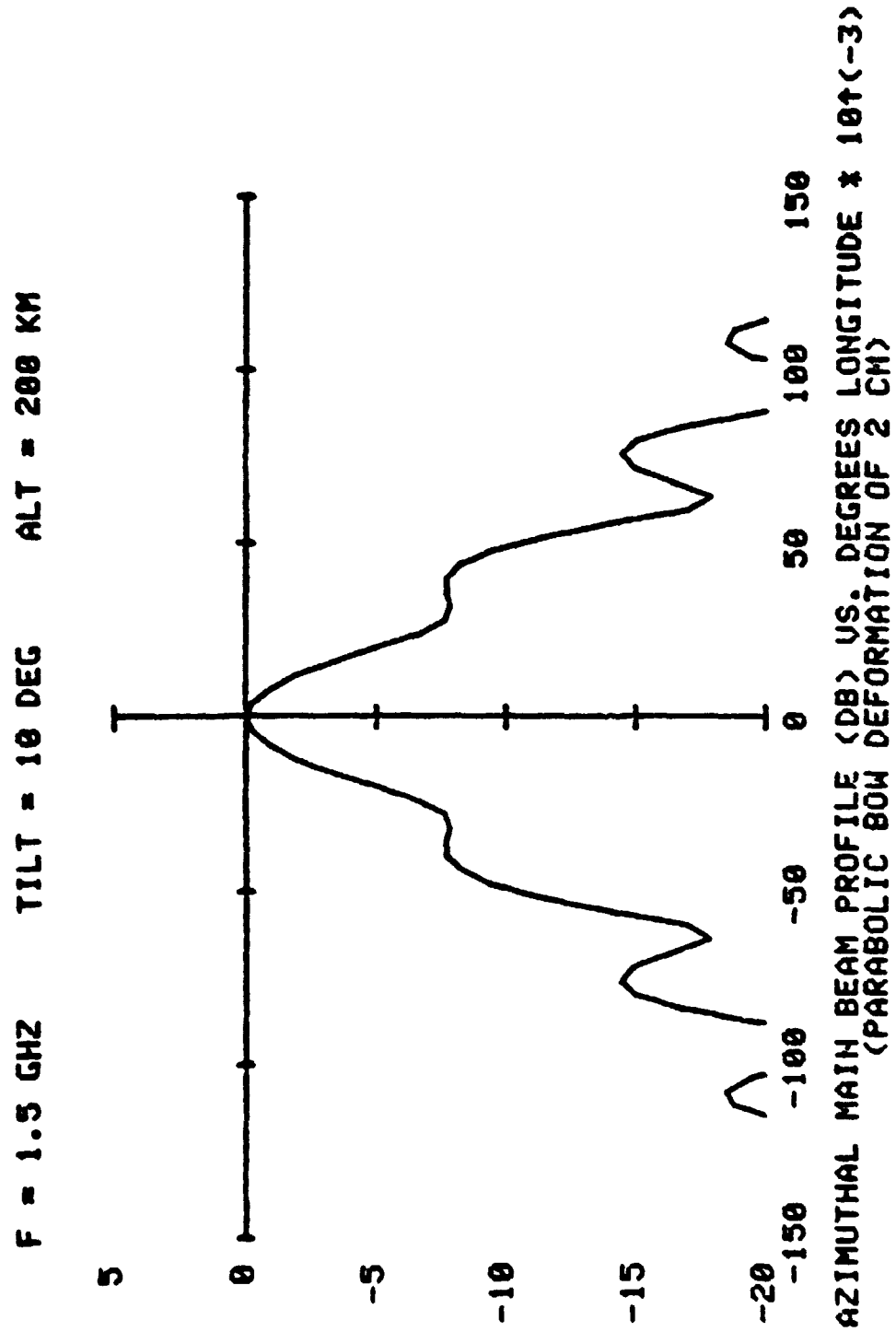


Figure 3.18 Azimuth main beam footprint profile.

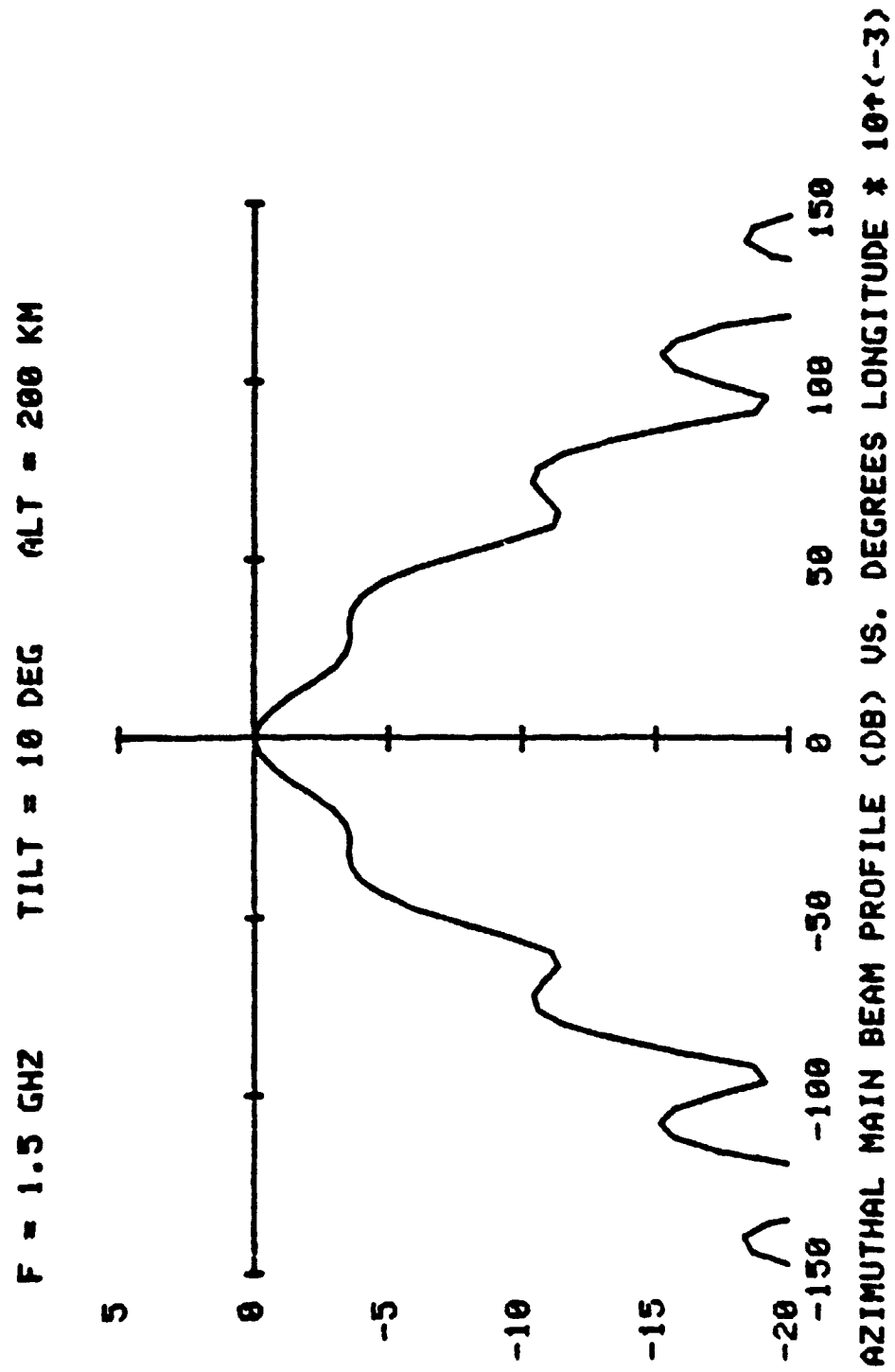


Figure 3.19 Azimuth main beam footprint profile.

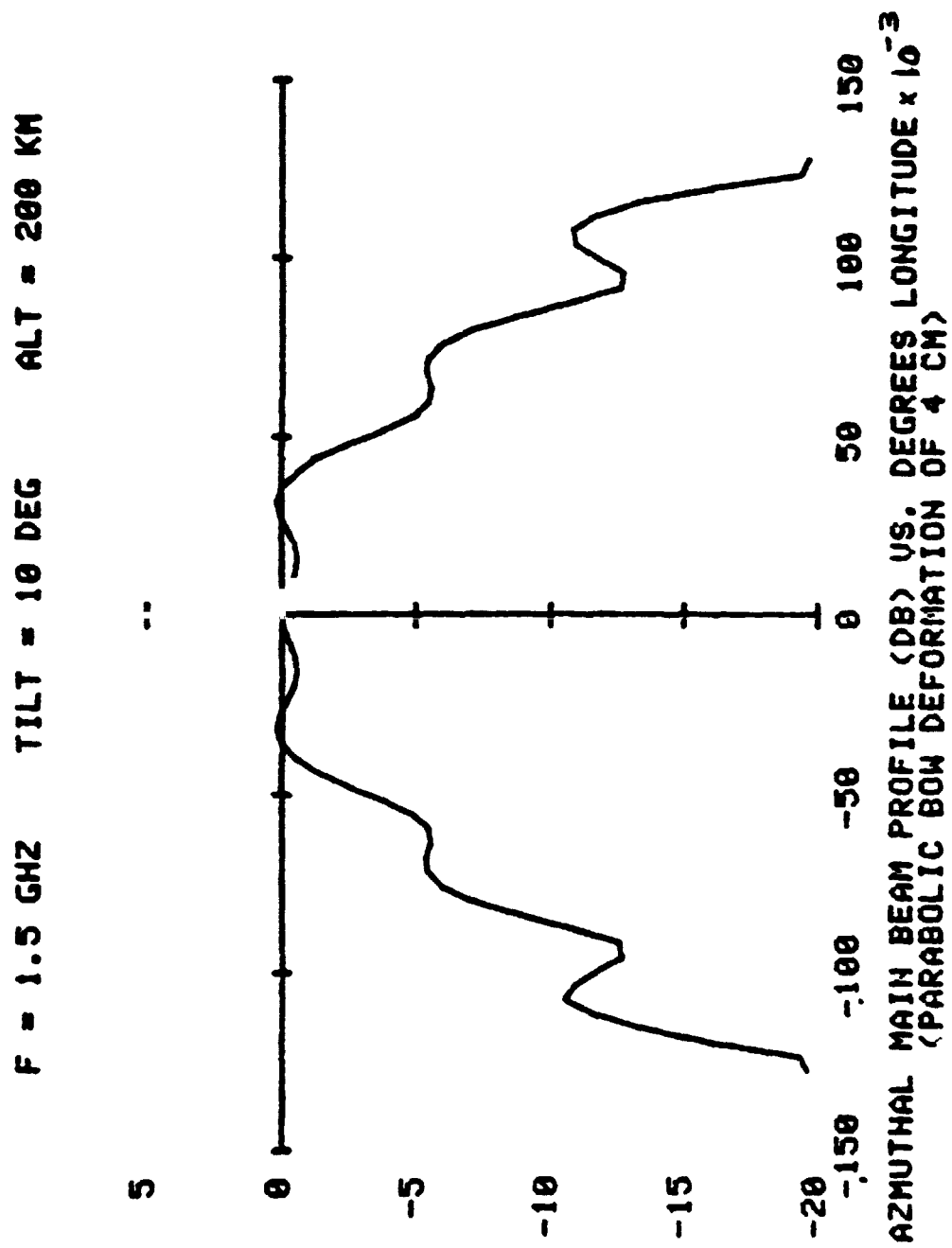


Figure 3.20 Azimuth main beam footprint profile.

Figures 3.21, 3.22, and 3.23 illustrate the effect of mechanical errors on azimuth SLL. (Since all errors thus far simulated were in the azimuth plane, the elevation SLL remained constant.)

### 3.5 Other Antenna Parameters

Two other antenna parameters will vary with mechanical/electrical deviations from flatness: (1) polarization purity and (2) cross-band/cross-polarization beam coincidence. These parameters, unlike the parameters discussed previously, depend upon the apportionment of space between frequencies and polarizations. These parameters will be investigated during Phase III.

### 3.6 Summary of Computer Predictions

From the simulations run thus far, it has been shown that minor errors in important antenna parameters, especially at the higher (X-band and up) frequencies will critically degrade antenna performance. Furthermore, the degradation in antenna performance increases rapidly for flatness errors greater than 2 cm (3/4"). A recent BBRC report<sup>2</sup> stated that deformations of up to 1/4" would have no measurable effect on antenna performance at L-band, but the report contained no substantiating data or patterns. In addition, BBRC has indicated in design review briefings that deflections of more than 1/4" are highly unlikely, though no physical justification was given. This indeed may be the case for the L-band SERGE antenna which has a strong-back monolithic mechanical structure; however, while the SIR-B support structure design has

---

<sup>2</sup> SERGE Antenna Concept Selection Review Report, NASA Contract NAS9-15363, August 3, 1977.

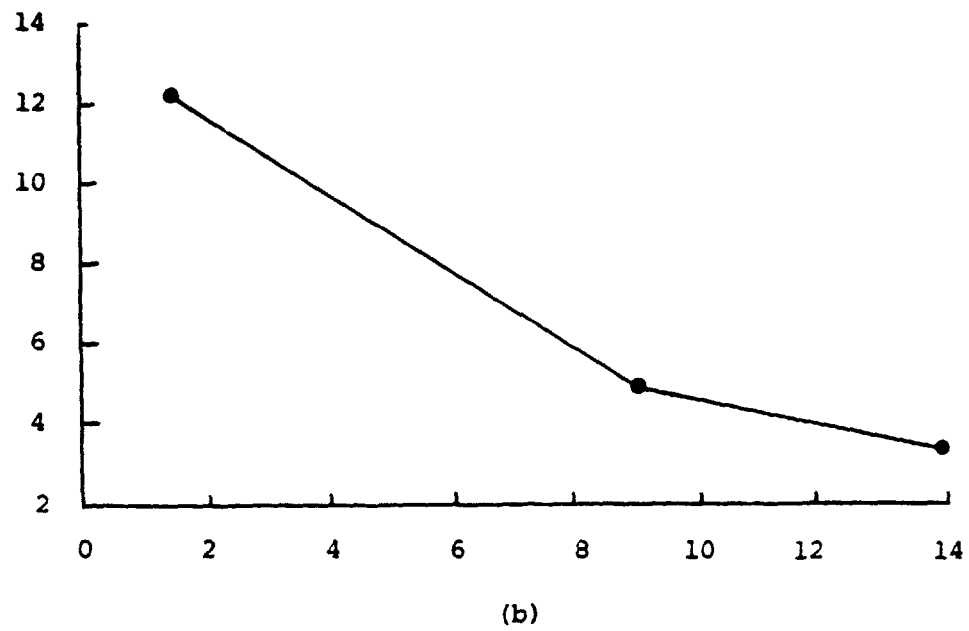
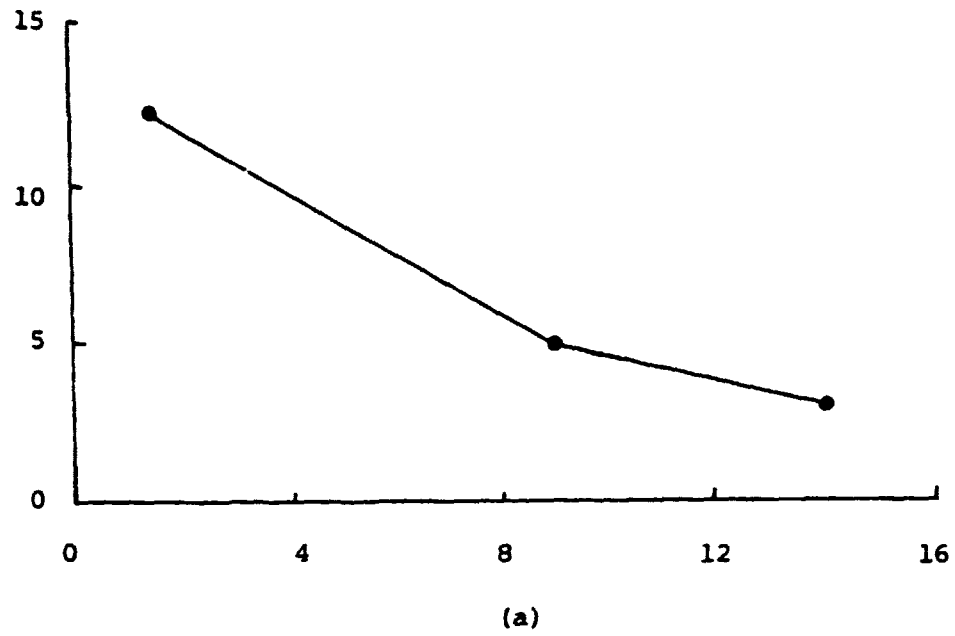
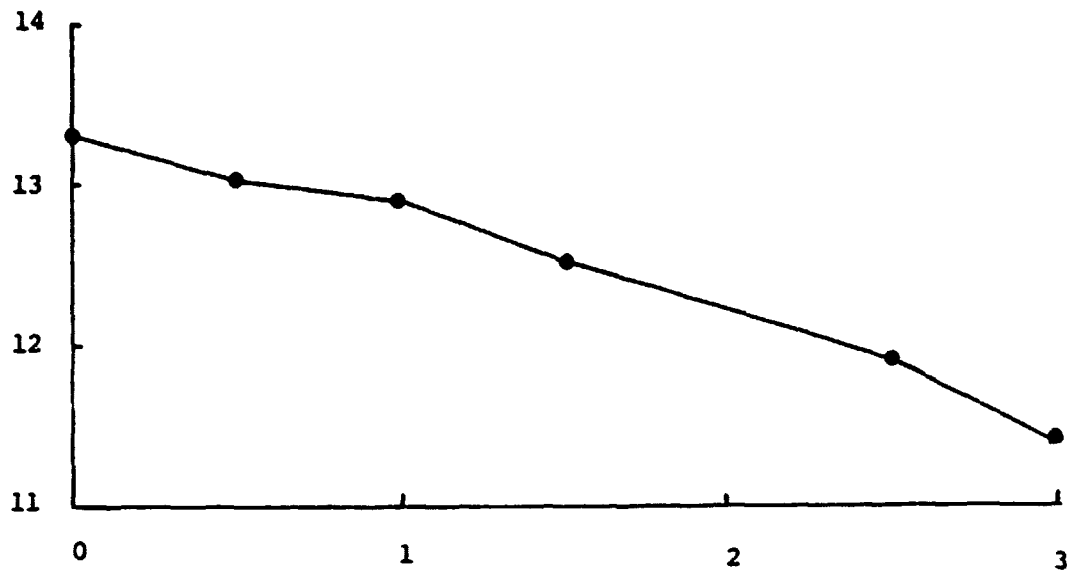
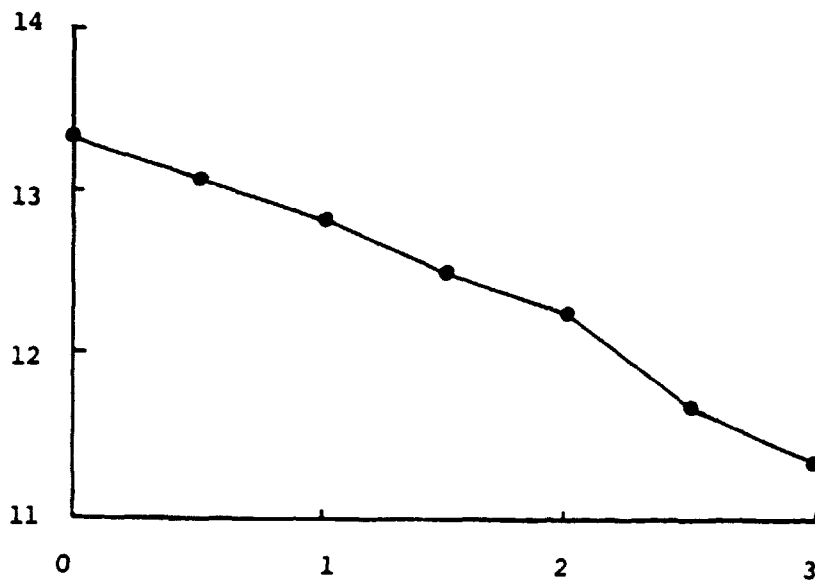


Figure 3.21. Side lobe level (dB) versus frequency (GHz) for panel unfolding errors at (a)  $10^\circ$  tilt, (b)  $50^\circ$  tilt.



(a)



(b)

Figure 3.22. Azimuth profile plane side lobe level (dB) versus warp severity for panel unfolding errors at 1.5 GHz: (a) 10° tilt, (b) 50° tilt.

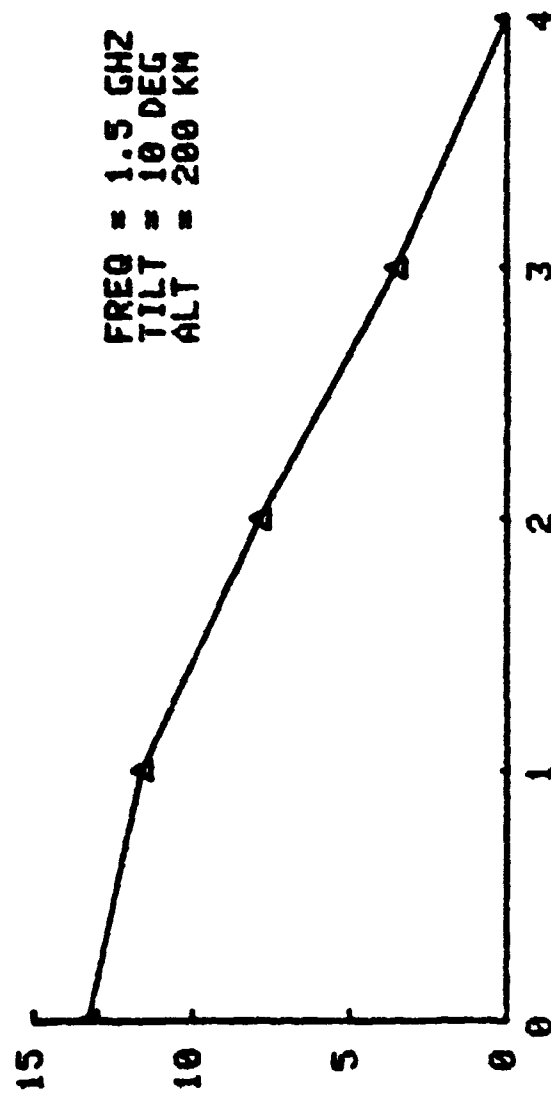


Figure 3.23 Azimuth profile plane side lobe level (DB) vs warp severity (CM)  
(parabolic bow deformation).

not yet been completed, it undoubtedly will be collapsible to fold and unfold from the shuttle payload bay.

Since the SERGE antenna will fly first, it is recommended that (1) further simulations of the SERGE antenna be performed to determine the maximum mechanical distortion which will still give acceptable antenna and processor operation, (2) the full-size SERGE antenna pattern and/or individual SERGE panel patterns be rigorously measured under possible mechanical deflections to support the computer predictions and (3) the 1/4" maximum deflection prediction be substantiated.

#### 4.0 FOOTPRINT CONTOUR MAPS OF FIFTEEN SIMULATIONS

Fifteen footprint maps from computer-generated data have been included to show the effects of frequency and error type on SIR antenna performance.

The following data were used in all simulations:

Yaw =  $0^\circ$

Tilt =  $50^\circ$

Twist =  $0^\circ$

Array Size:  $11.6 \text{ m} \times 8 \frac{1}{2} \lambda$

Illumination: Uniform

Subsatellite Point:  $0^\circ$  Lat.,  $0^\circ$  Long.

Contour Region:  $-1/2 \leq \text{Lat.} \leq 1/2$ ,  $0 \leq \text{Long.} \leq 4$  degrees

Computer Plot Resolution:  $151 \times 151$  points

The following simulations are shown:

<u>Figure</u>	<u>Frequency (GHz)</u>	<u>Error Type</u>
4.1	1.5	None
4.2	1.5	Panel Unfolding Error
4.3	1.5	Parabolic Bow Error
4.4	4.5	None
4.5	4.5	Panel Unfolding Error
4.6	4.5	Parabolic Bow Error
4.7	9.0	None
4.8	9.0	Panel Unfolding Error
4.9	9.0	Parabolic Bow Error
4.10	12.0	None
4.11	12.0	Panel Unfolding Error
4.12	12.0	Parabolic Bow Error
4.13	14.0	None
4.14	14.0	Panel Unfolding Error
4.15	14.0	Parabolic Bow Error

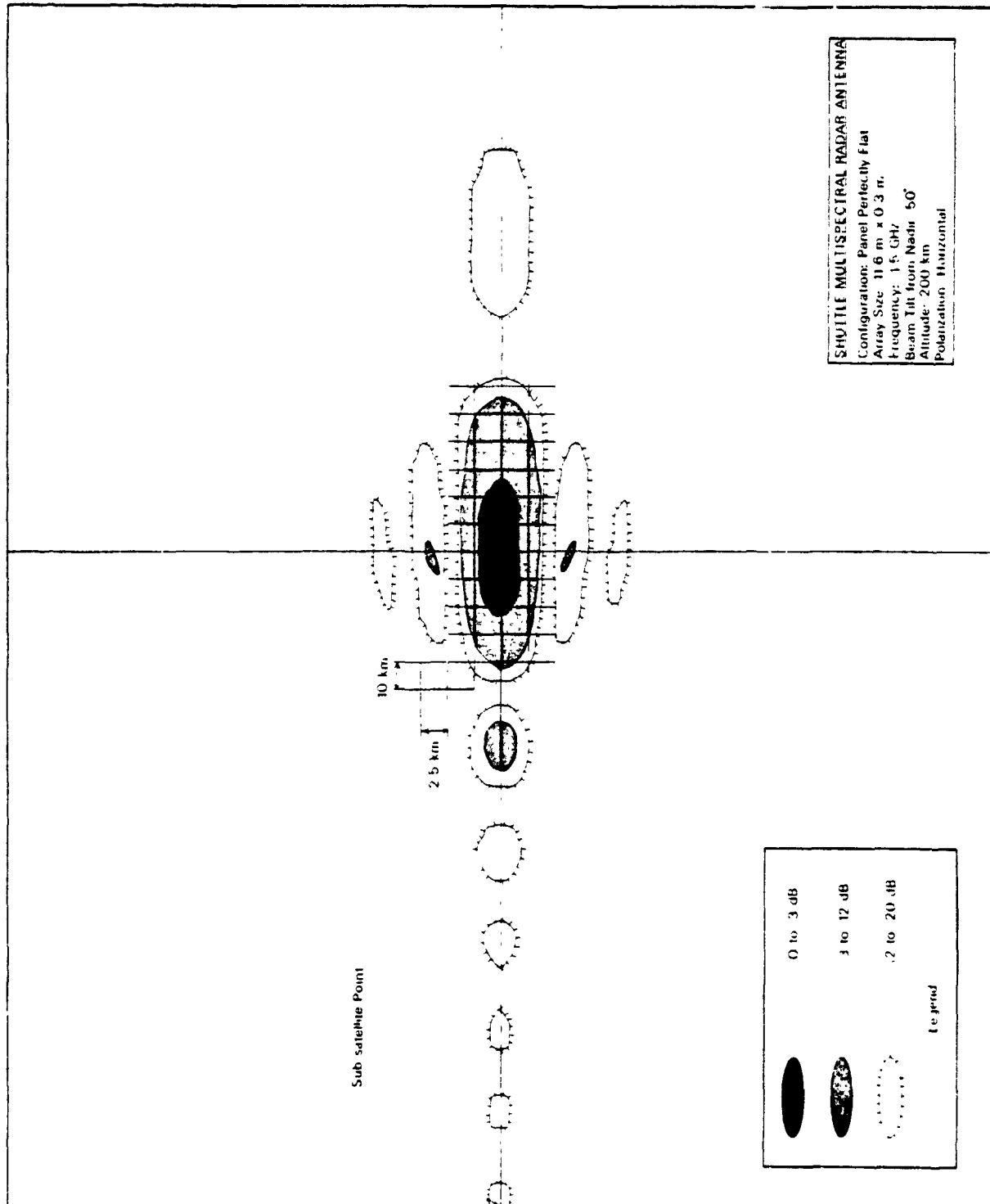


Figure 4.1

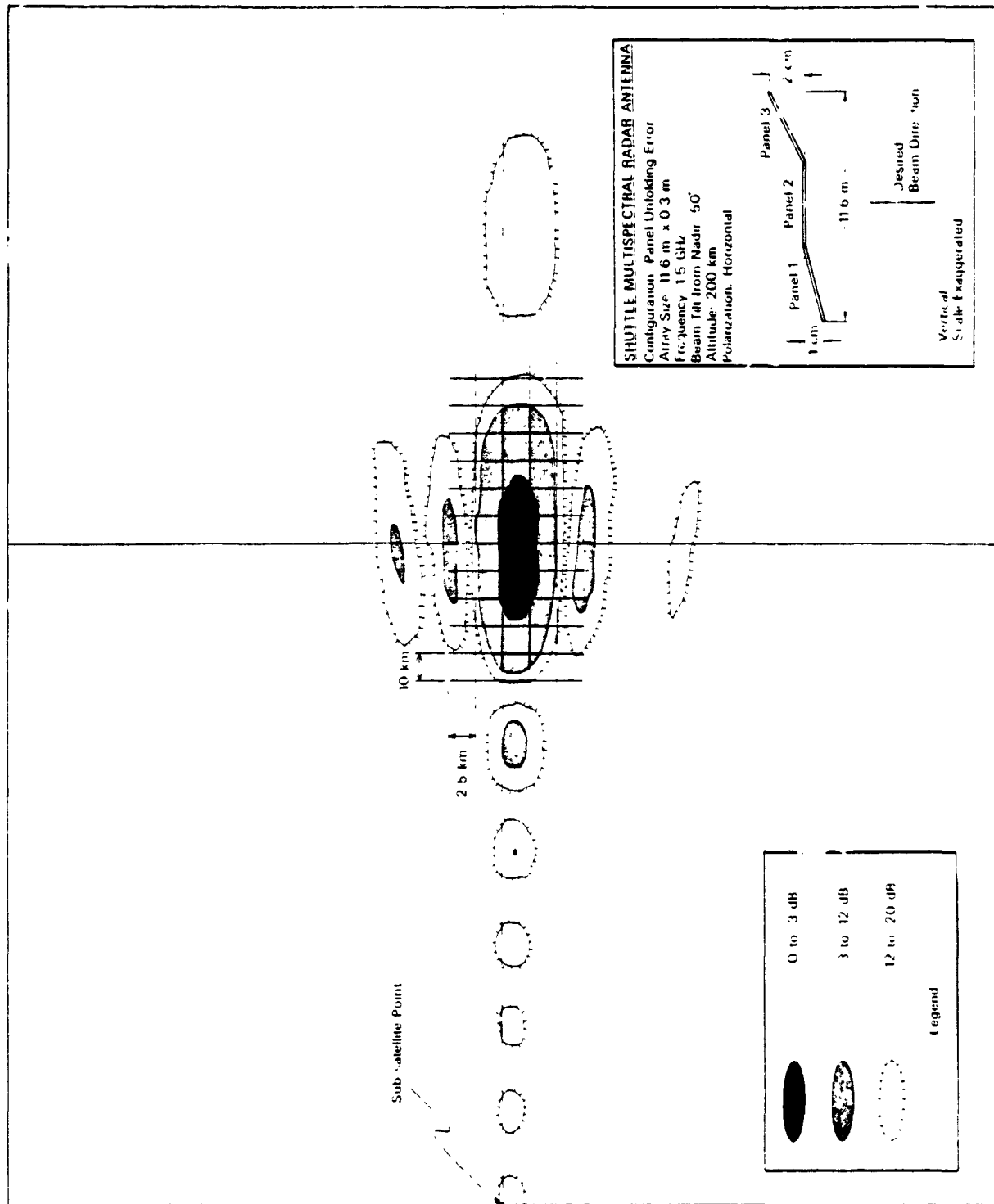


Figure 4.2

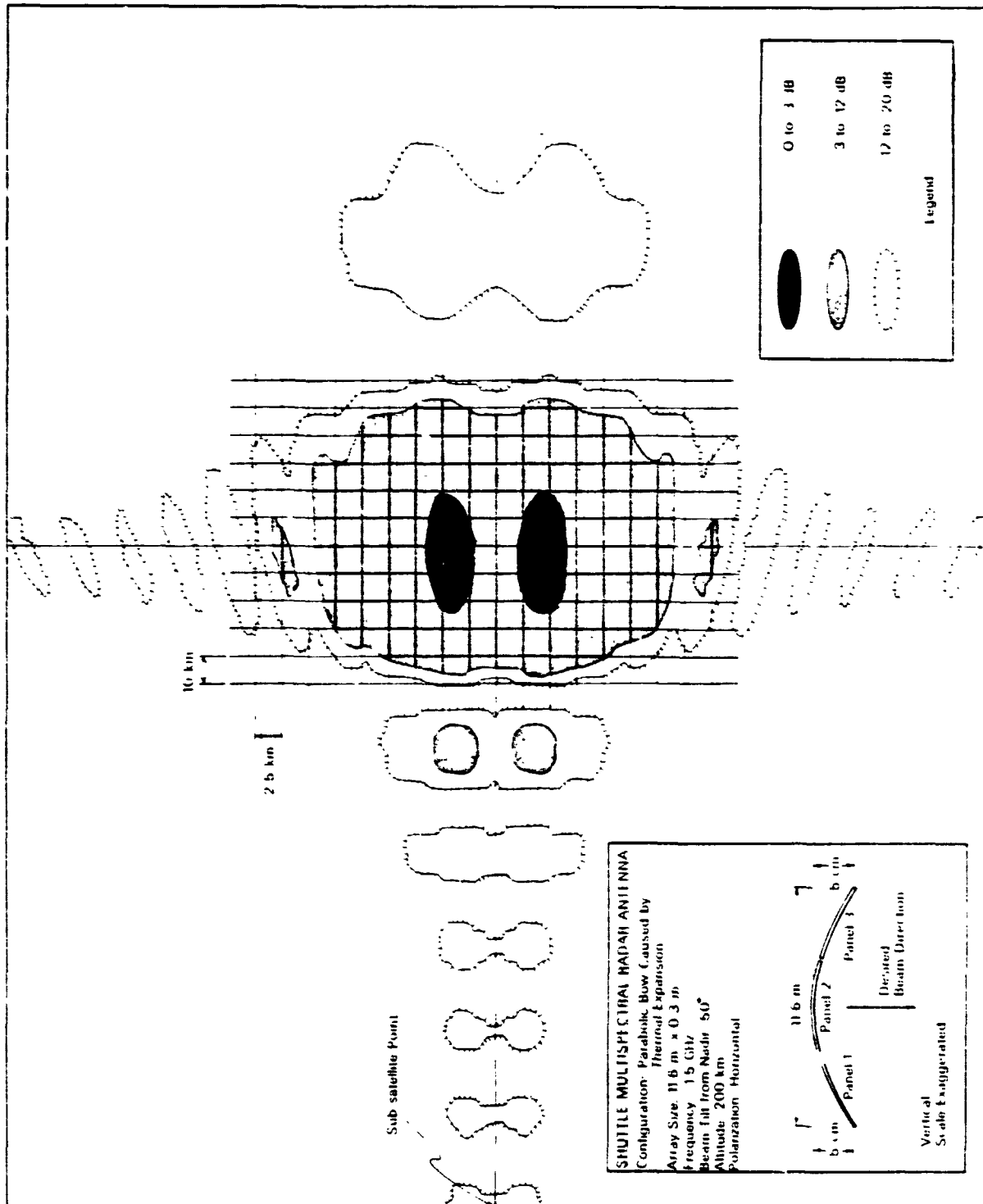


Figure 4.3

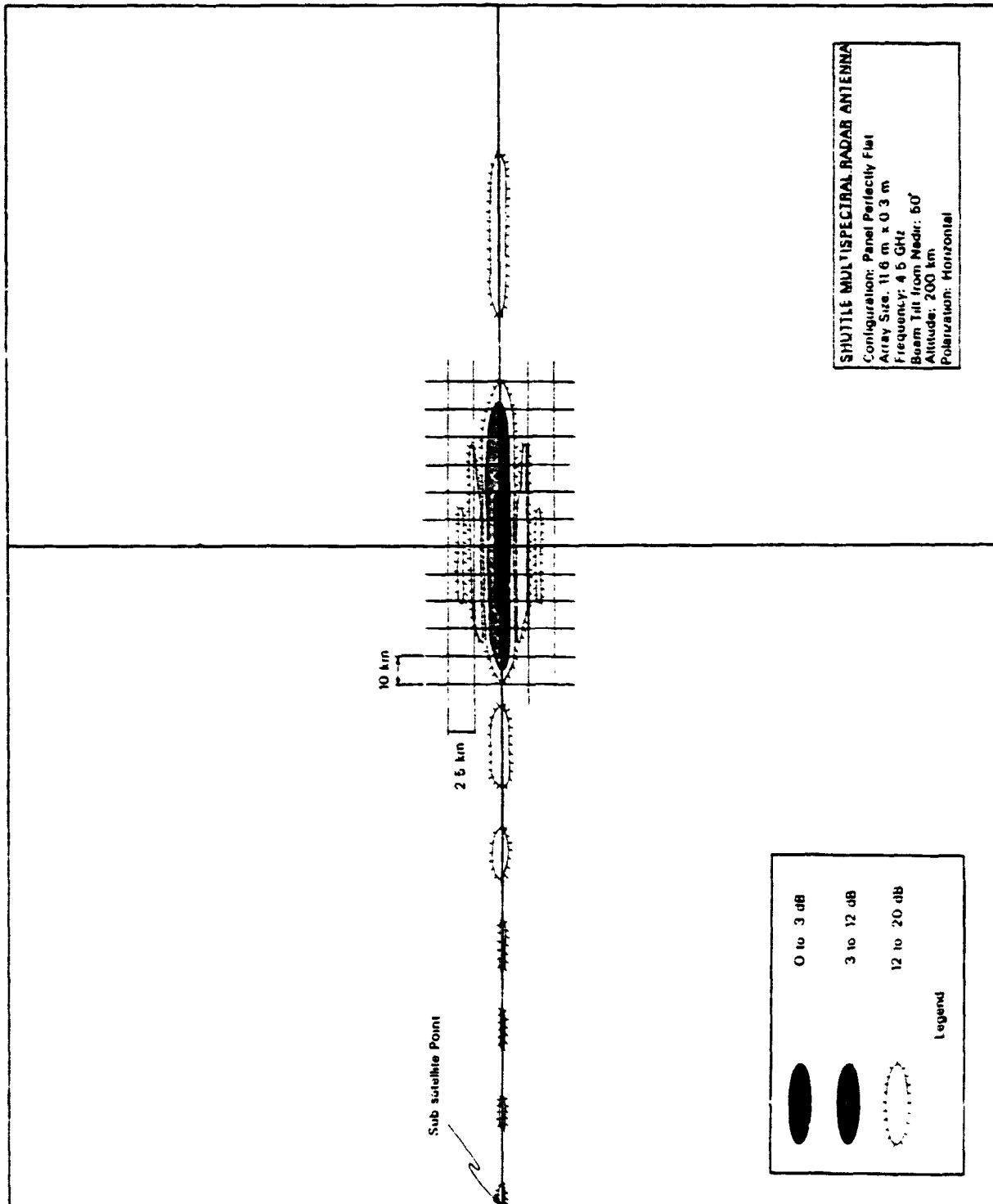


Figure 4.4

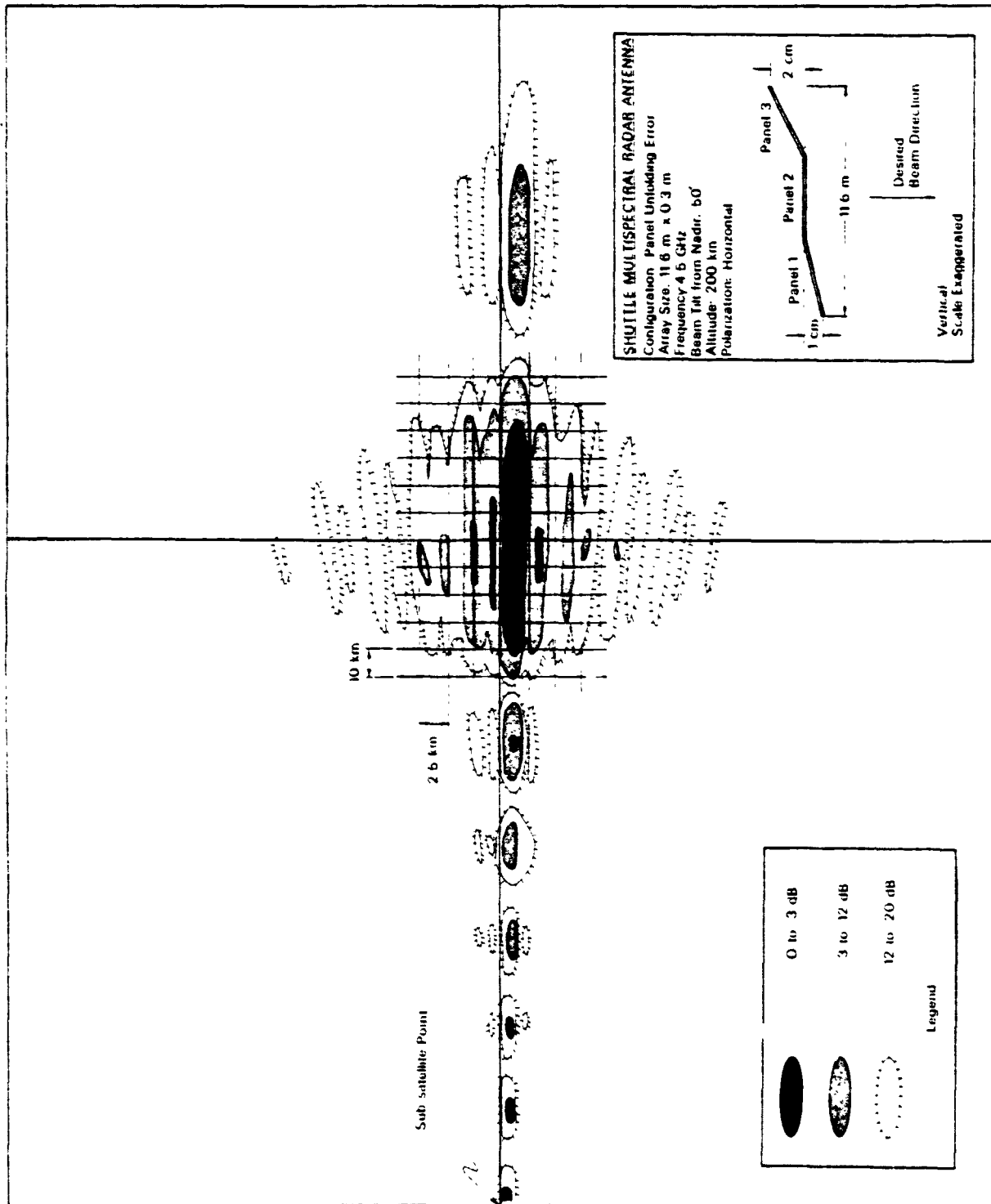


Figure 4.5

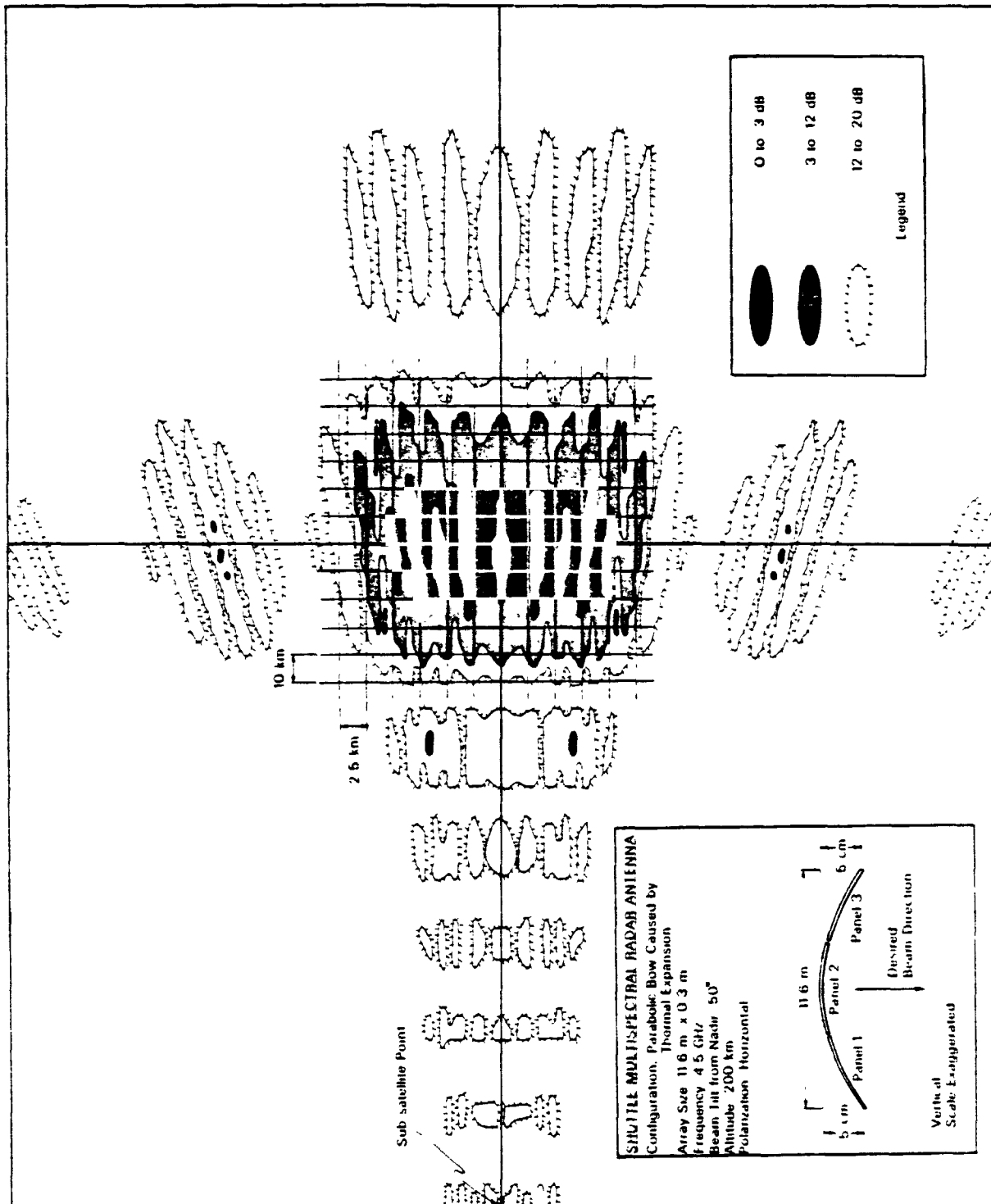


Figure 4.6

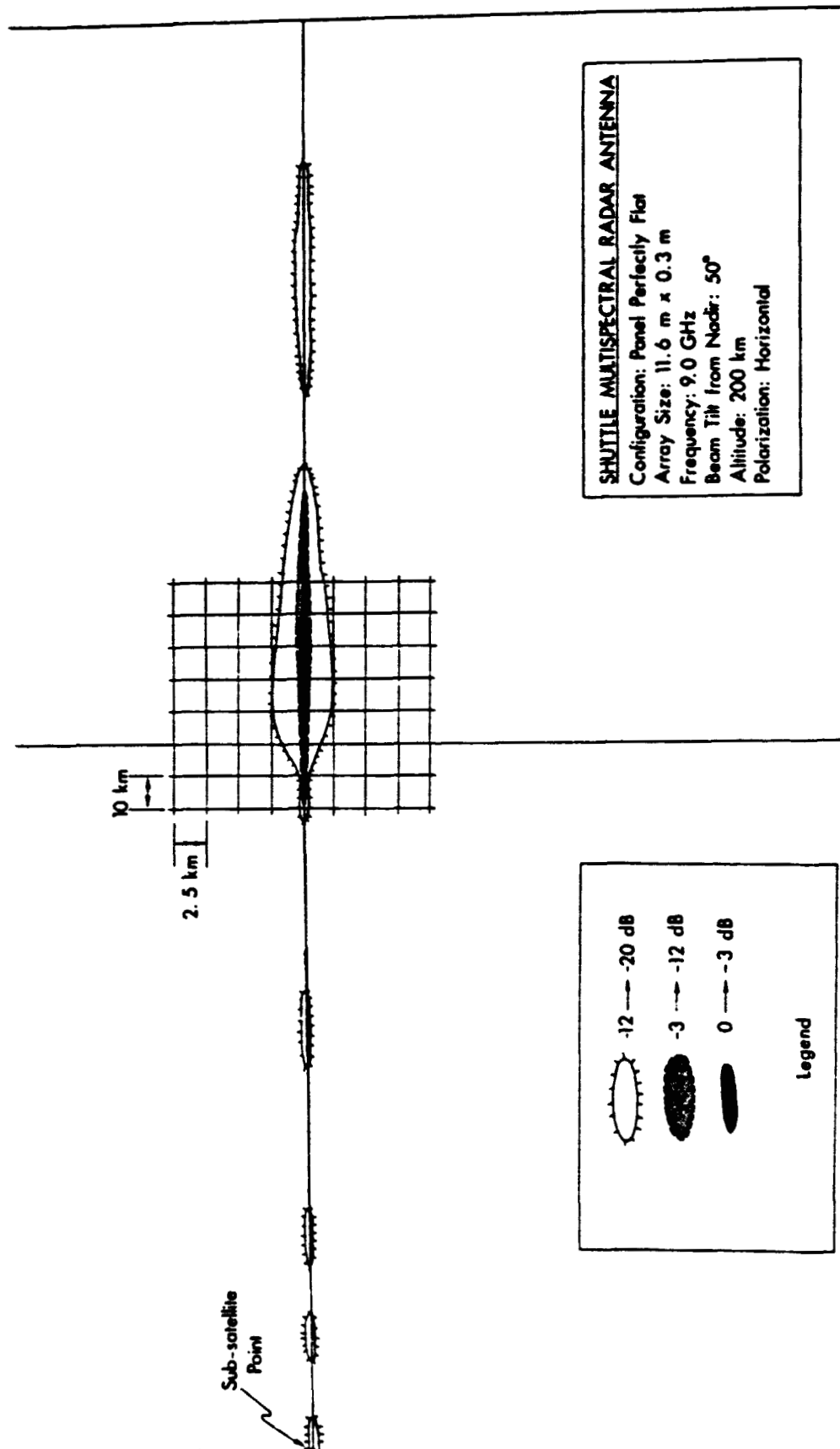


Figure 4.7

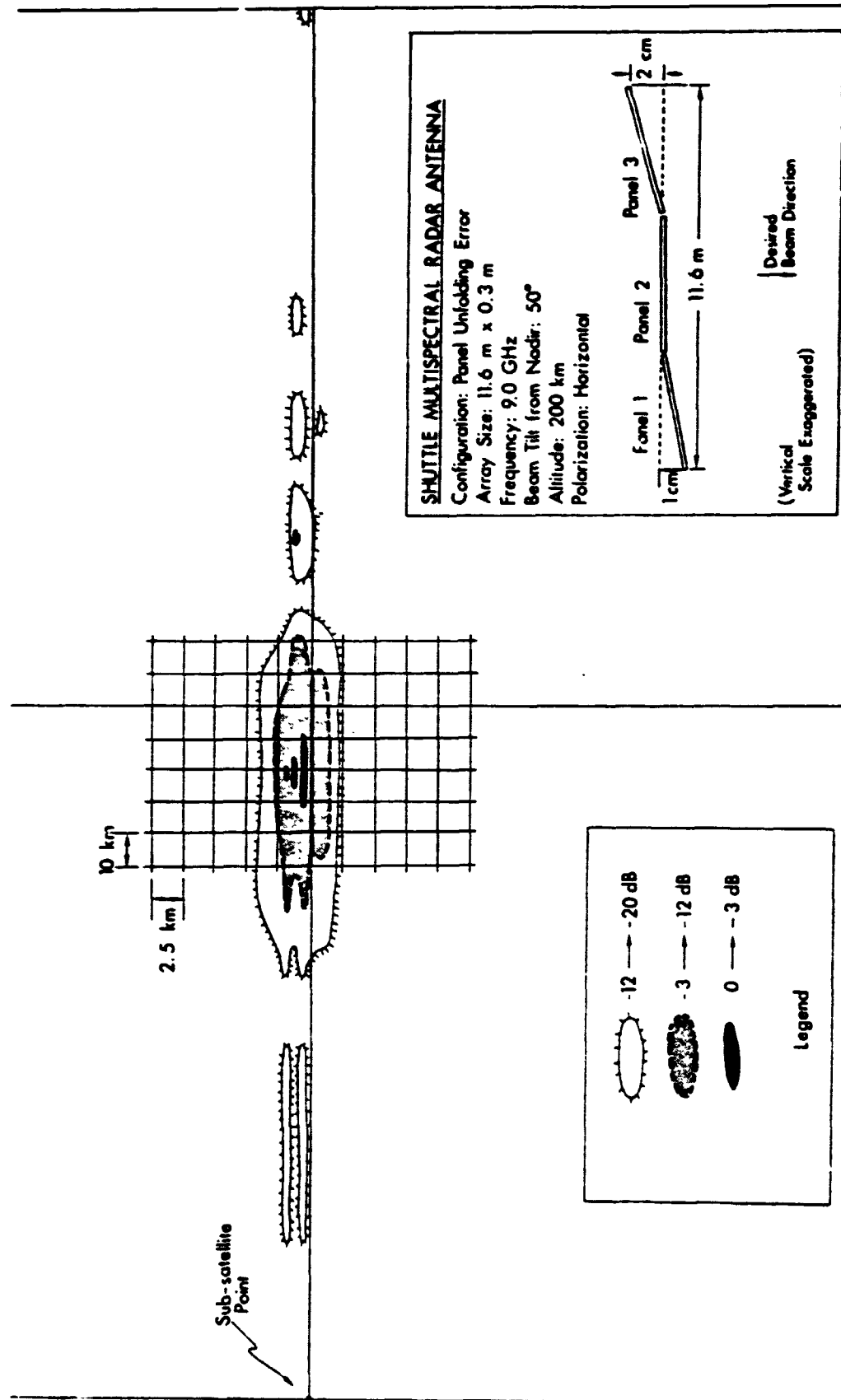


Figure 4.8

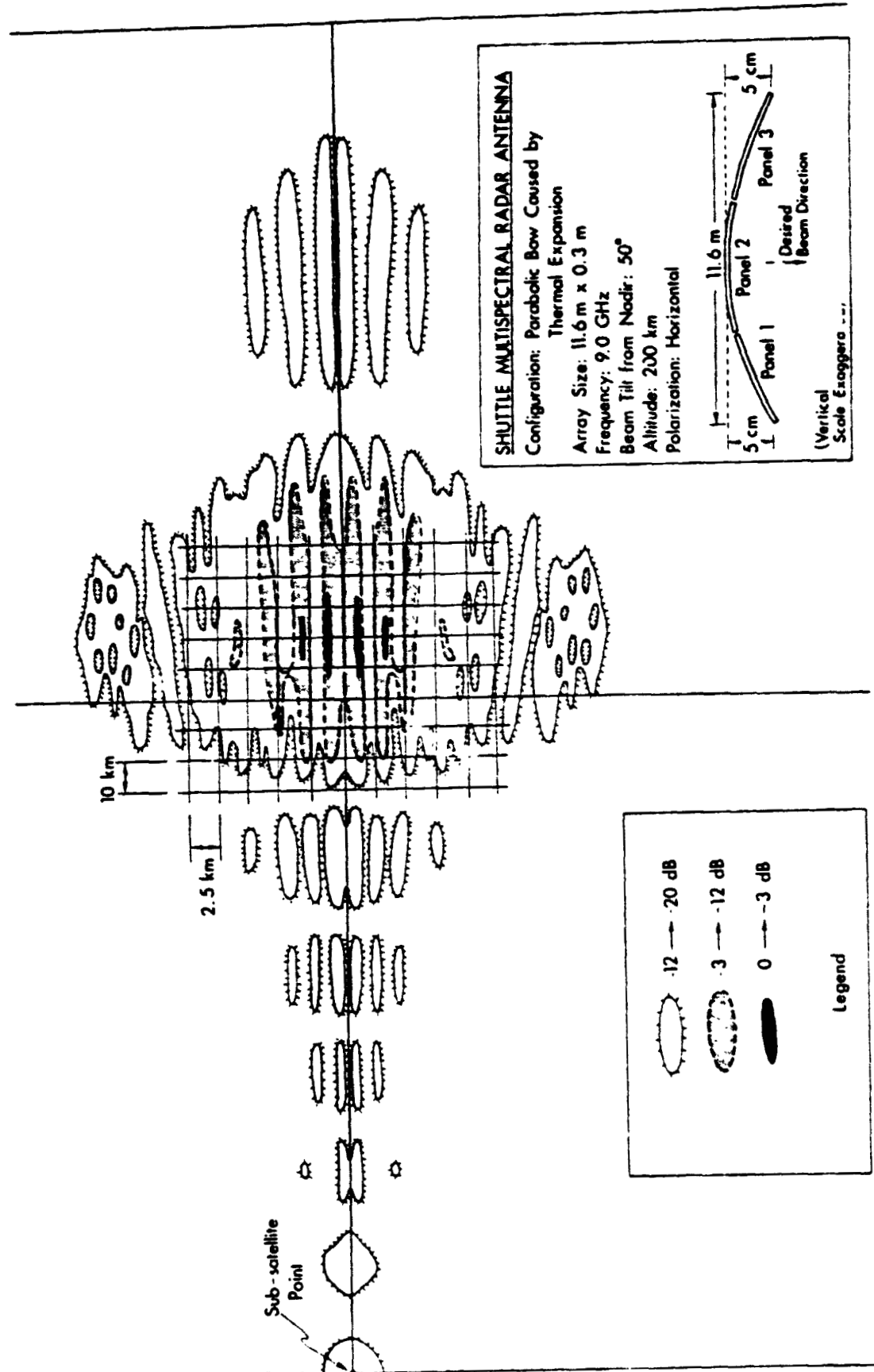


Figure 4.9

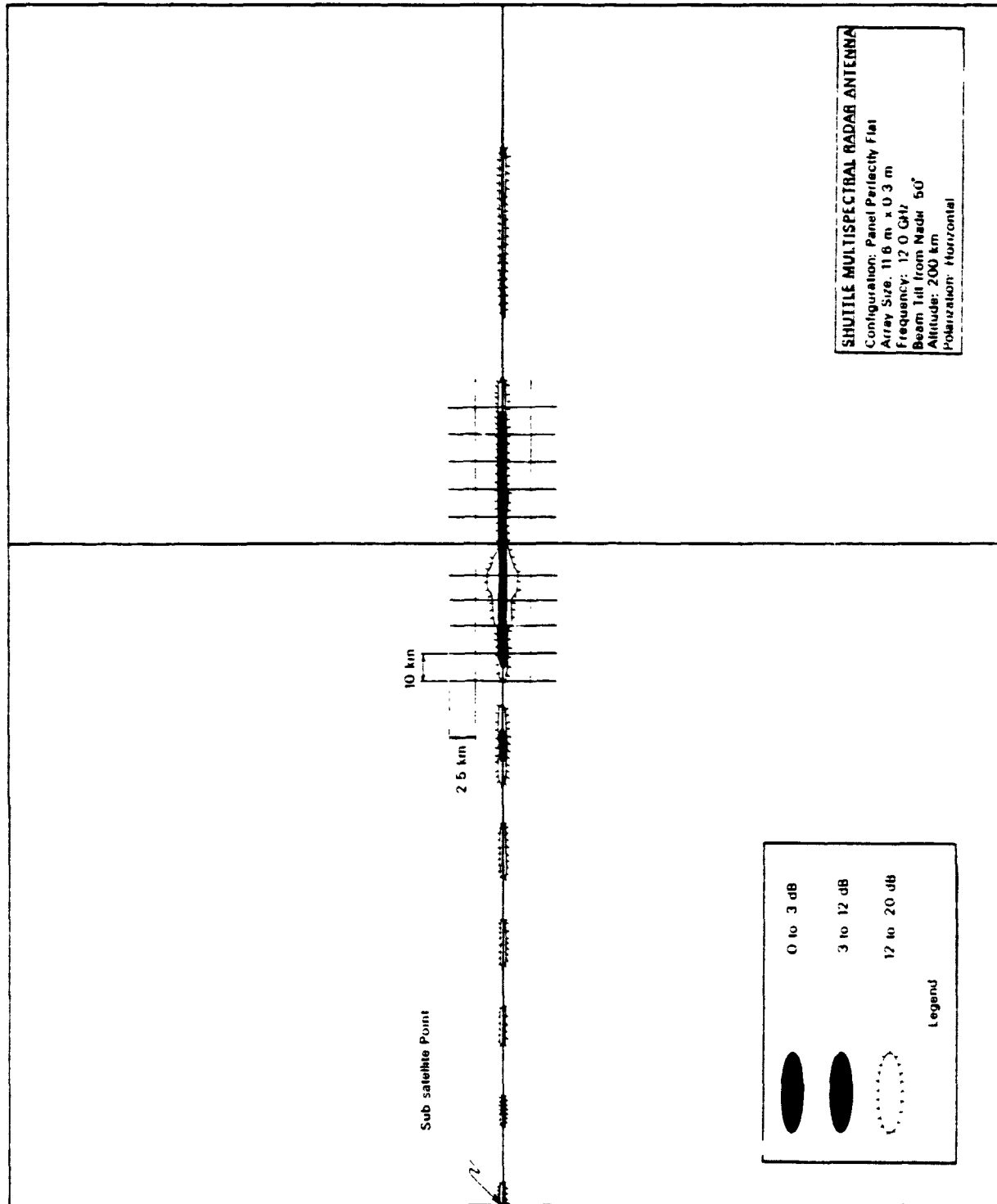


Figure 4.10

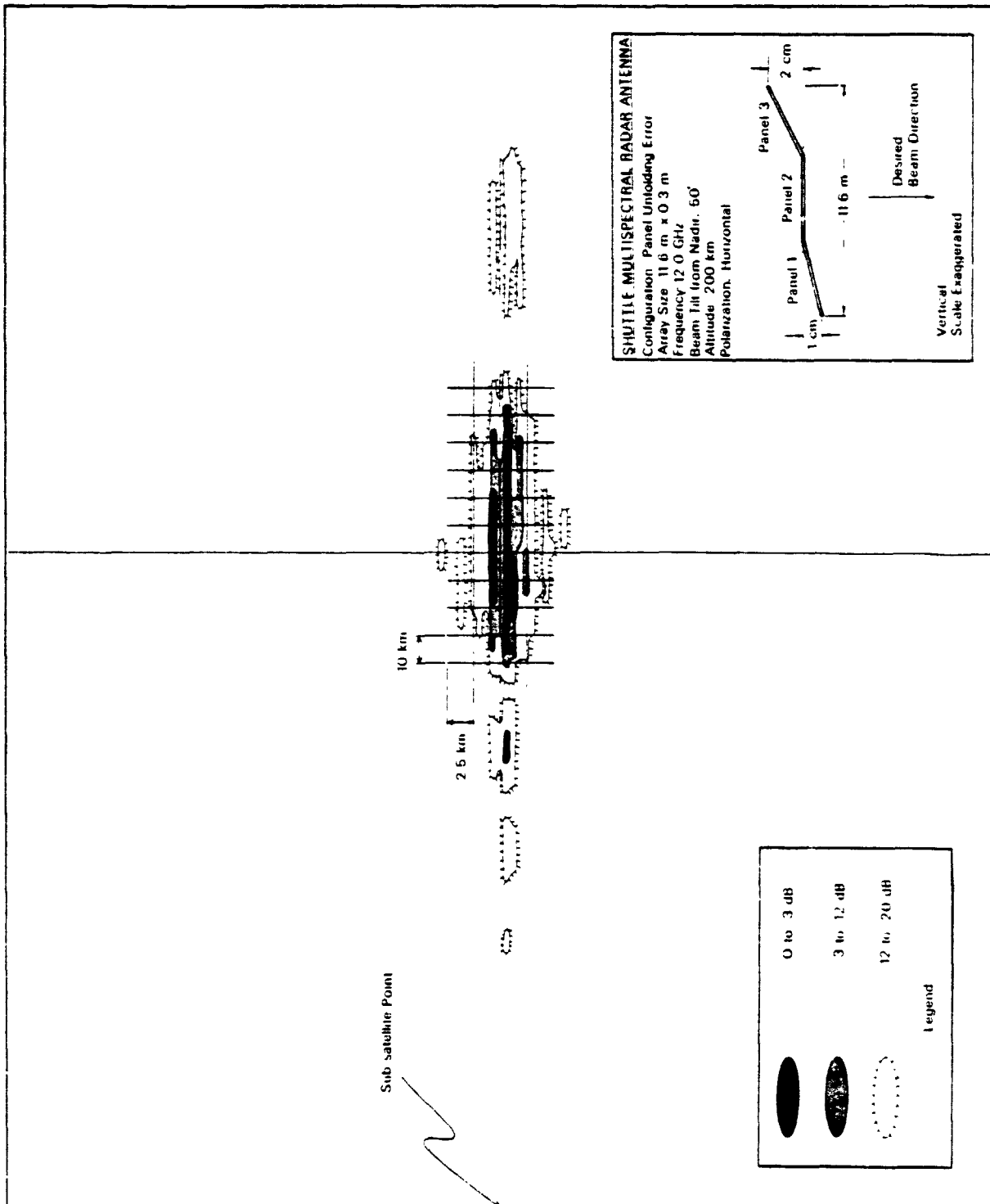


Figure 4.11

ORIGINAL PAGE IS  
OF POOR QUALITY

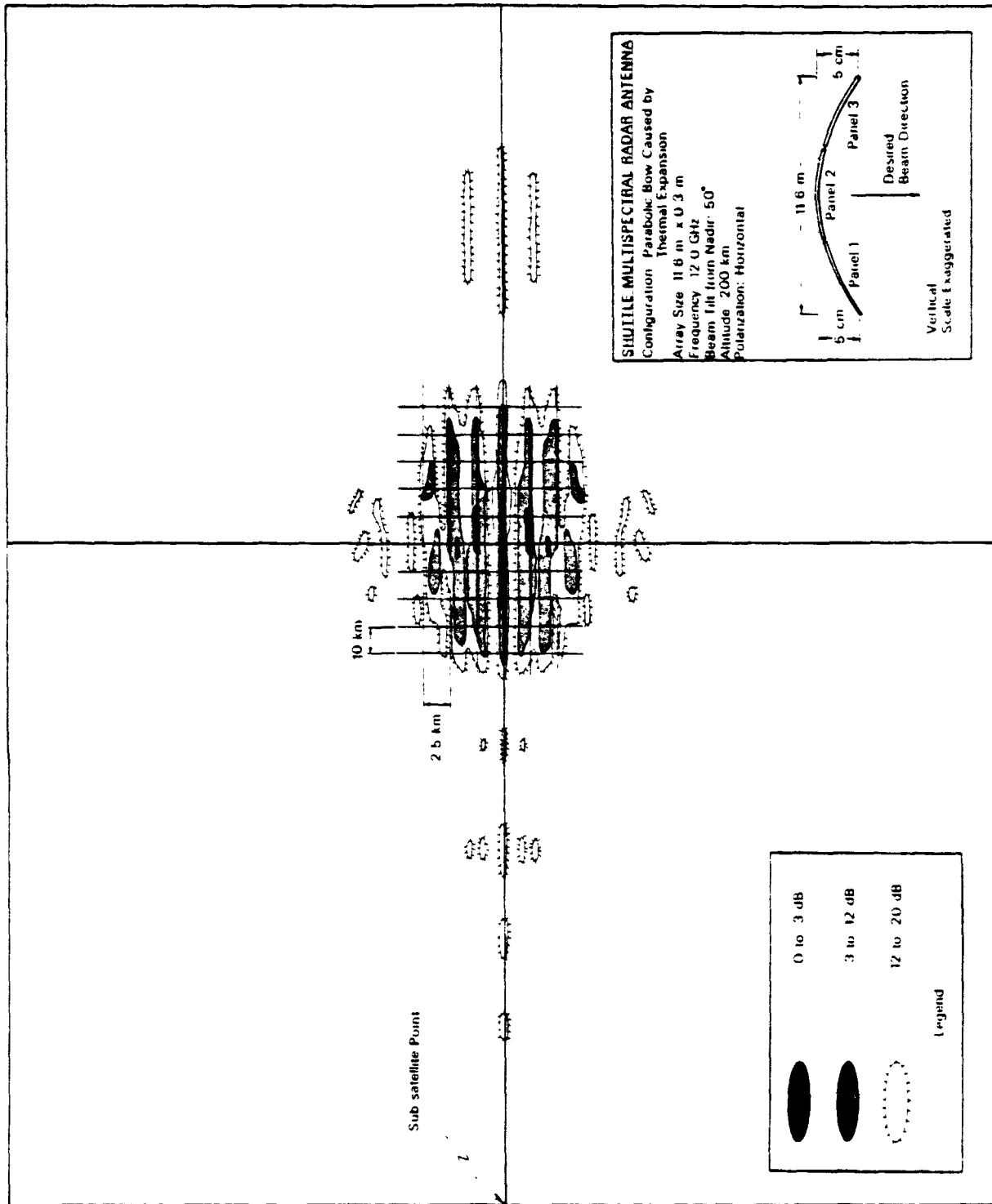


Figure 4.12

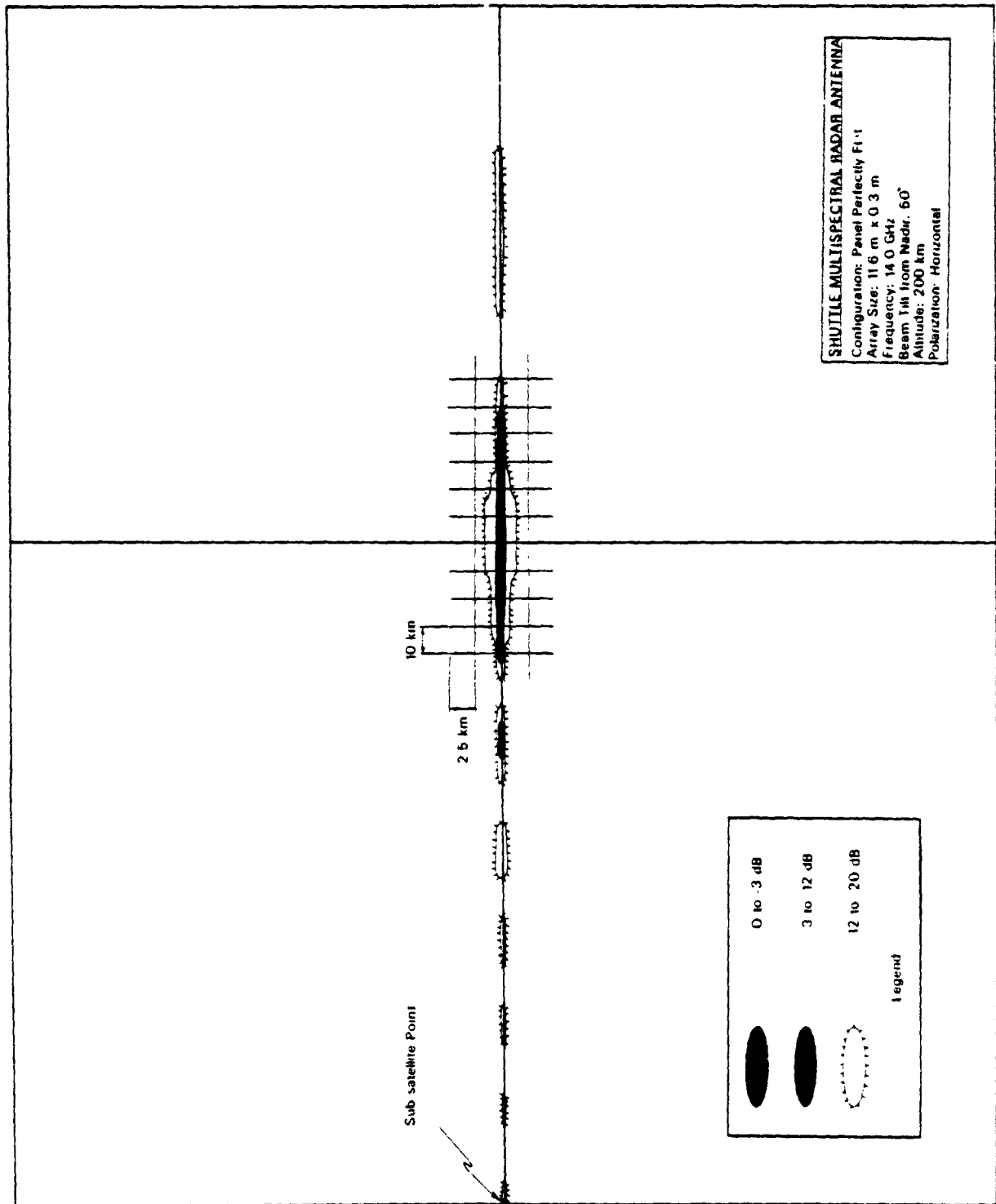


Figure 4.13

ORIGINAL PAGE IS  
OF POOR QUALITY

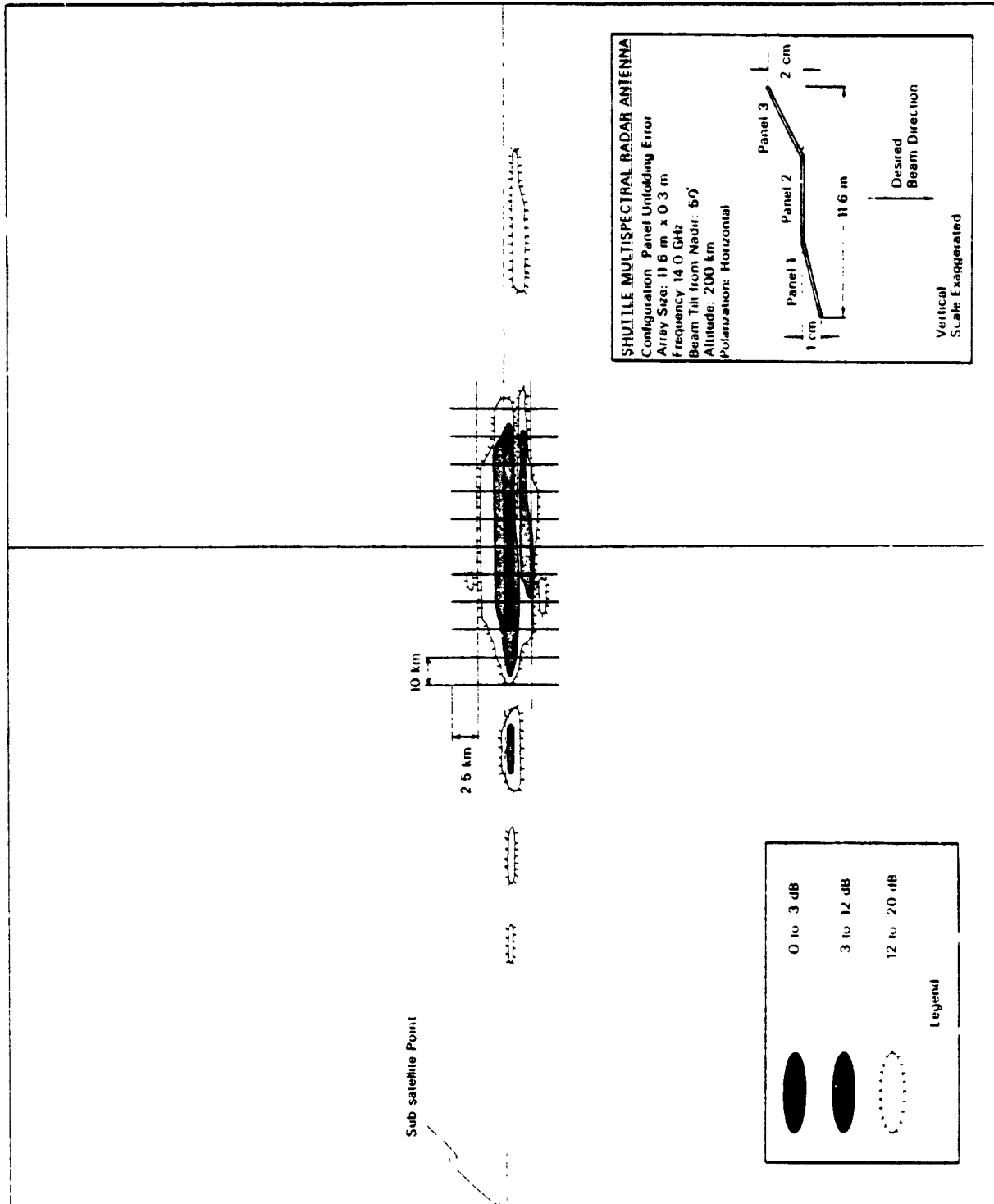


Figure 4.14

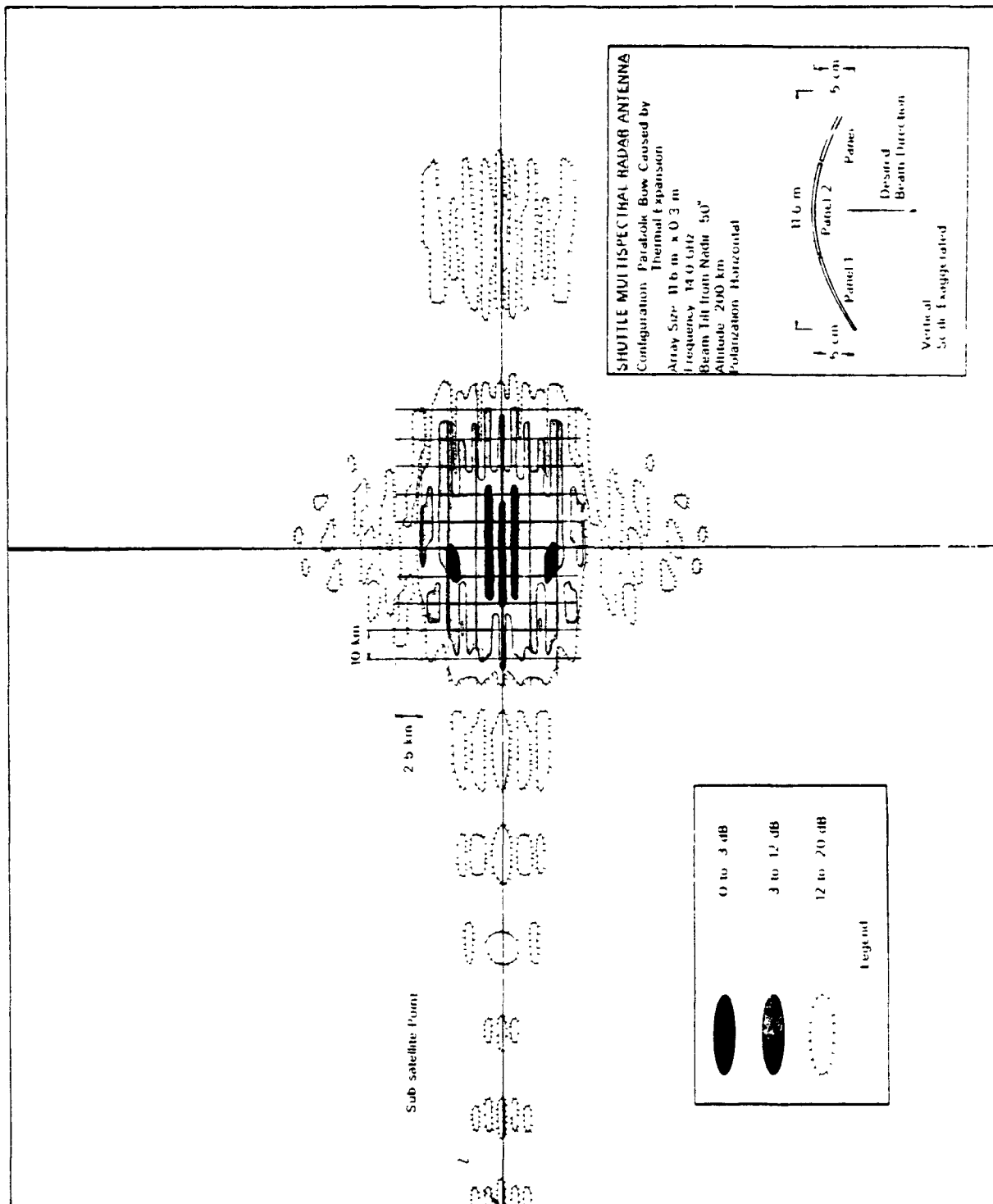


Figure 4.15